

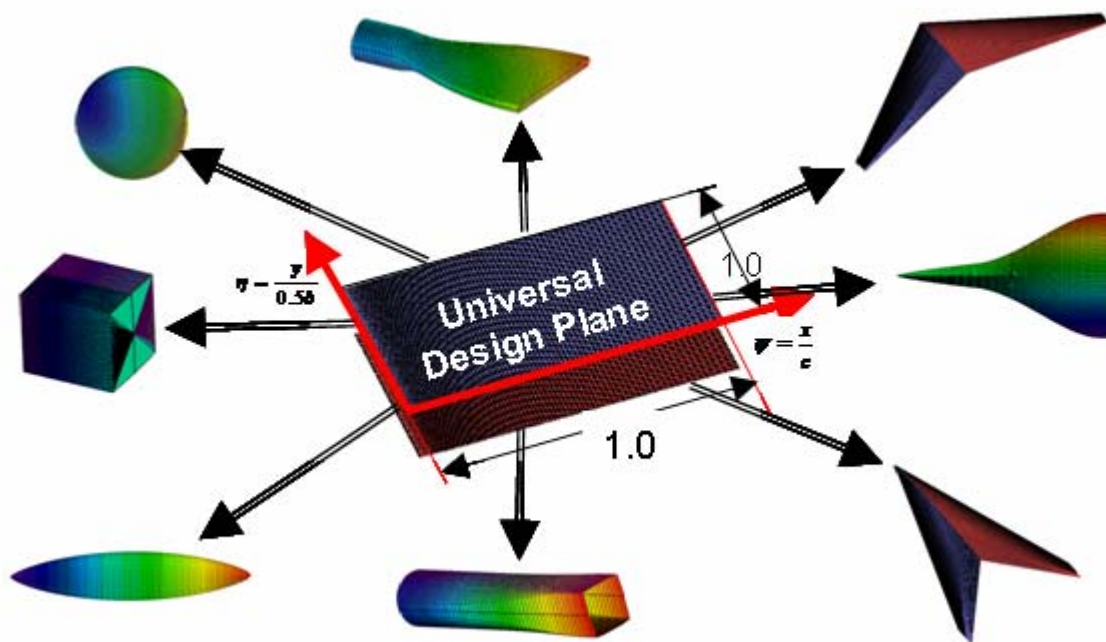


AIAA--2007-0062

## A Universal Parametric Geometry Representation Method – “CST”

Brenda M. Kulfan

*Boeing Commercial Airplane Group, Seattle, Washington, 98124*



**45th AIAA Aerospace Sciences Meeting and Exhibit**

**8 - 11 Jan 2007  
Reno Hilton  
Reno, Nevada**

Copyright © 2006 by Boeing Commercial Airplanes.

Published by the American Institute of Aeronautics and Astronautics, Inc., with permission.

American Institute of Aeronautics and Astronautics

# A Universal Parametric Geometry Representation Method – “CST”

Brenda M. Kulfan\*

*Boeing Commercial Airplane Group, Seattle, Washington, 98124*

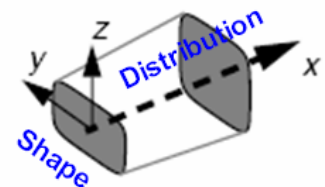
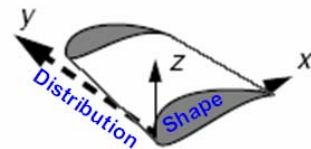
For aerodynamic design optimization, it is very desirable to limit the number of the geometric design variables. In reference 1, a “fundamental” parametric airfoil geometry representation method was presented. The method included the introduction of a geometric “shape function / class function” transformation technique such that round nose / sharp aft end geometries as well as other classes of geometries could be represented exactly by analytic well behaved and simple mathematical functions having easily observed physical features. The fundamental parametric geometry representation method was shown to describe an essentially limitless design space composed entirely of analytically smooth geometries. In this paper, the “shape function / class function” methodology is extended to more general three dimensional applications such as wing, body, ducts and nacelles. It is shown that any general 3D geometry can be represented by a distribution of fundamental shapes, and that the “shape function / class function” methodology can be used to describe the fundamental shapes as well as the distributions of the fundamental shapes. The “CST” method of representing 3D geometries is introduced. With this very robust, versatile and simple method, a 3D geometry is defined in a design space by the distribution of class functions and the shape functions. This design space geometry is then transformed into the physical space in which the actual geometry is defined. A number of applications of the “CST” method to nacelles, ducts, wings and bodies are presented to illustrate the versatility of this new methodology. It is shown that relatively few numbers of variables are required to represent arbitrary 3D geometries such as an aircraft wing, nacelle or body.

## I. Introduction

The fundamental aerodynamic definition of any aircraft consists of representing the basic defining components of the configuration by utilizing two fundamental types of shapes<sup>2</sup> together with the distribution of the shapes along each of the components.

The two fundamental defining shapes include:

- Class 1: Wing airfoil type shapes that define such components as:
  - Airfoils
  - Aircraft wings
  - Helicopter rotors
  - Turbomachinery blades
  - Horizontal and vertical tails, canards
  - Winglets
  - Pylons / struts
  - Nacelles (defined by streamwise profiles)
- Class 2: Body cross-section type shapes that define such components as:
  - Aircraft fuselages (cross sections)
  - Rotor hubs and shrouds
  - Channels, ducts and tubing
  - Axisymmetric bodies
  - Lifting Bodies
  - Nacelles (when defined by cross sections)



\* Engineer/Scientist – Technical Fellow, Enabling Technology & Research, PO Box 3707, Seattle, WA 98124 / MS 67-LF, AIAA Member.

The particular design features of the defining shapes are indeed quite dependent on the application as well as the flow environment especially the cruise Mach number. In some very highly integrated configurations such as hypersonic wave riders, the individual components may not be readily discernible. Some components such as nacelles may be defined utilizing either of the two fundamental types. For example, a nacelle may be defined with airfoil type sections that are distributed circumferentially around the nacelle centerline. A nacelle could also be defined by body type cross-sections that are distributed along the axis of the nacelle.

A previous paper<sup>1</sup> focused on the class 1 type of 2D airfoil shapes that have a round nose and a pointed aft-end. A new and powerful methodology for describing such geometries was presented. In the current paper, the methodology is extended to represent class II geometries as well as to general 3D geometries.

A brief description and review of the methodology presented in the previous paper will be shown since knowledge of this information is essential to the understanding of the extension of the methodology that is presented in the present paper.

The concept of representing arbitrary 3D geometries as distribution of fundamental shapes is discussed. It is shown that the previously method developed for 2D airfoils and axi-symmetric bodies or nacelles, can be used to mathematically describe both the fundamental shapes as well as the distribution of the shapes for rather arbitrary 3D geometries. Applications of the extended methodology to a variety of 3D geometries including wings and nacelles are shown.

## II. Round Nose Airfoil Representation

A typical subsonic wing airfoil section is shown in figure 1. Round nose airfoils such as shown in the figure, have an infinite slope and an infinite 2nd derivative at the leading edge and large variations in curvature over the airfoil surface. The mathematical description of an airfoil must therefore deal with a rather complex non-analytic function over the surface of the airfoil. Consequently a large number of “x,z” coordinates are typically required along with a careful choice of interpolation techniques in order to provide a mathematical or numerical description of the surfaces of a cambered airfoil.

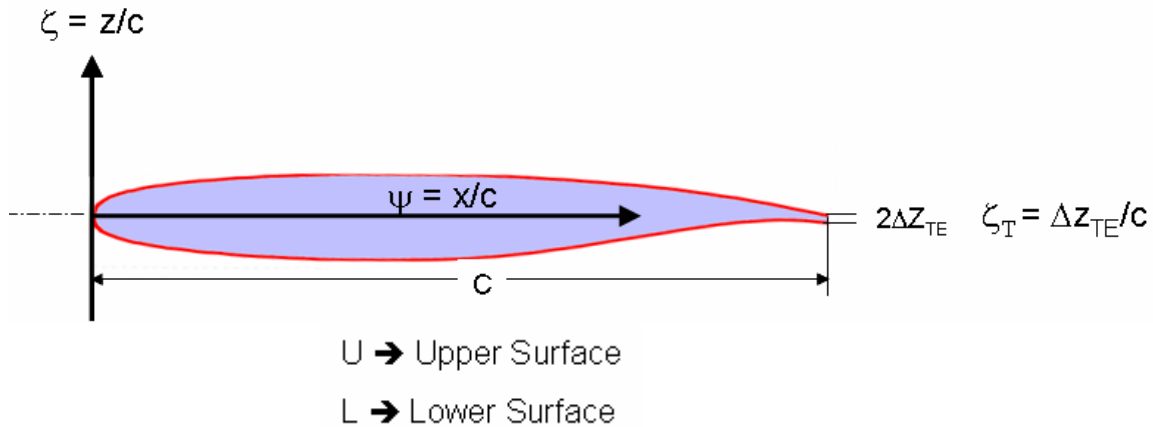


Figure 1: Typical Wing Airfoil Section

The choice of the mathematical representation of an airfoil, that is utilized in any particular aerodynamic design optimization process, along with the selection of the type of optimization algorithm have a profound effect on such things as:

- Computational time and resources
- The extent and general nature of the design space that determines whether or not the geometries contained in the design space are smooth or irregular, or even physically realistic or acceptable
- If a meaningful “optimum” is even contained in the design space
- If optimum designs exist, whether or not they can they be found.

The method of geometry representation also affects the suitability of the selected optimization process. For example the use of discrete coordinates as design variables may not be suitable for use with a genetic optimization process since the resulting design space could be heavily populated with airfoils having bumpy irregular surfaces, thus making the possibility of locating an optimum smooth practically impossible.

Desirable design features for any geometric representation technique include:

- Well behaved and produces smooth and realistic shapes
- Mathematically efficient and numerically stable process that is fast, accurate and consistent
- Flexibility
  - Requires relatively few variables to represent a large enough design space to contain optimum aerodynamic shapes for a variety of design conditions and constraints
  - Allows specification of key design parameters such as leading edge radius, boat-tail angle, airfoil closure.
  - Provide easy control for designing and editing the shape of a curve
- Intuitive - Geometry algorithm should have an intuitive and geometric interpretation.
- Systematic and Consistent - The way of representing, creating and editing different types of curves (*e.g.*, lines, conic sections and cubic curves) must be the same.
- Robust - The represented curve will not change its geometry under geometric transformations such as translation, rotation and affine transformations.

Commonly used geometry representation methods typically fail to meet the complete set of desirable features<sup>1</sup>.

### III. Mathematical Description of Airfoil Geometry

The approach used in reference 1 to develop an improved airfoil geometry representation method is based on a technique that the author has often used successfully in the past, to develop effective computational methods to deal with numerically difficult functions.

In the case of the round nose airfoil described in a fixed Cartesian coordinate system, the slopes and 2<sup>nd</sup> derivatives of the surface geometry are infinite at the nose and large changes in curvature occur over the entire airfoil surface. The mathematically characteristics of the airfoil surfaces are therefore non-analytic function with singularities in all derivatives at the nose.

The technique used to develop an efficient well behaved method to geometrically describe such geometry involved the following steps:

1. Develop a general mathematical equation necessary and sufficient to describe the geometry of any round nose / sharp aft end airfoil;
2. Examine the general nature of this mathematical expression to determine the elements of the mathematical expression that are the source of the numerical singularity
3. Rearrange or transform the parts of the mathematical expression to eliminate the numerical singularity.
4. This resulted in identifying and defining a “shape function” transformation technique such that the “design space” of an airfoil utilizing this shape function becomes a simple well behaved analytic function with easily controlled key physical design features in addition to possessing an inherent strong smoothing capability.
5. Subsequently a “Class Function” was introduced to generalize the methodology for applications to a wide variety of fundamental 2D airfoils and axi-symmetric nacelle and body geometries.

A summary of this approach is discussed below.

The general and necessary form of the mathematical expression that represents the typical airfoil geometry shown in figure 1 is:

$$\zeta(\psi) = \sqrt{\psi} \cdot (1 - \psi) \cdot \sum_{i=0}^N A_i \cdot \psi^i + \psi \cdot \zeta_T \quad (1)$$

Where:  $\psi = x/c$      $\zeta = z/c$     and     $\zeta_T = \Delta\zeta_{TE}/c$ .

The term  $\sqrt{\psi}$  is the only mathematical function that will provide a round nose.

The term  $(1 - \psi)$  is required to insure a sharp trailing edge.

The term  $\psi \cdot \zeta_T$  provides control of the trailing edge thickness.

The term  $\sum_{i=0}^{\infty} A_i \psi^i$  represents a general function that describes the unique shape of the geometry between the round nose and the sharp aft end.

This term is shown for convenience as a power series but it can be represented by any appropriate well behaved analytic mathematical function.

#### IV. Airfoil Shape Function

The source of the non-analytic characteristic of the basic airfoil equation is associated with the square root term in equation 1.

Let us define the shape function “S(ψ)” that is derived from the basic geometry equation by first subtracting the base area term and then dividing by the round nose and sharp end terms.

This gives:

$$S(\psi) \equiv \frac{\zeta(\psi) - \psi \zeta_T}{\sqrt{\psi} \cdot [1 - \psi]} \quad (2)$$

The equation that represents the “S” function which is obtained from equations 1 and 2 becomes the rather simple expression:

$$S\left(\frac{x}{L}\right) = \sum_{i=0}^N \left[ A_i \cdot \left[ \frac{x}{L} \right]^i \right] \quad (3)$$

The “shape function” equation is a simple well behaved analytic equation for which the “eye” is well adopted to see the represented detailed features of an airfoil and to make critical comparisons between various geometries.

It was shown in reference 1, that the nose radius, the trailing edge thickness and the boat-tail angle are directly related to the unique bounding values of the “S(ψ)” function.

The value of the shape function at  $x/c = 0$  is directly related to the airfoil leading edge nose radius by the relation:

$$S(0) = \sqrt{2 R_{LE} / C} \quad (4)$$

The value of the shape function at  $x/c = 1$  is directly related to the airfoil boat-tail angle,  $\beta$ , and trailing edge thickness,  $\Delta Z_{te}$ , by the relation:

$$S(1) = \tan \beta + \frac{\Delta Z_{te}}{C} \quad (5)$$

Hence, in the transformed coordinate system, specifying the endpoints of the “S” function provide and an easy way to define and to control the leading edge radius, the closure boat-tail angle and trailing edge thickness.

An example of the transformation of the actual airfoil geometry to the corresponding shape function is shown in figure 2. The transformation of the constant  $Z_{max}$  height line, and the constant boat-tail angle line, are also shown as curves in the transformed plane.

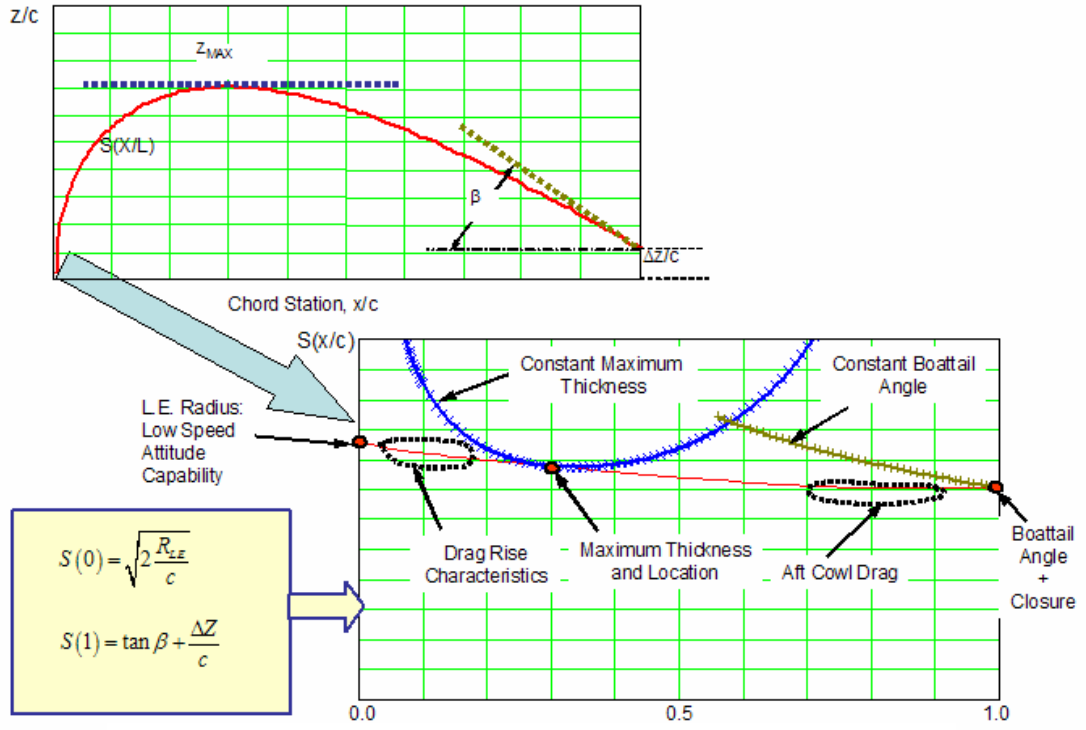


Figure 2: Example of an Airfoil Geometric Transformation

The shape function for this example airfoil is seen to be approximately a straight line with the value at zero related to the leading edge radius of curvature and the value at the aft end equal to tangent of the boat-tail angle plus the ratio of trailing edge thickness / chord length. It is readily apparent that the shape function is indeed a very simple analytic function.

The areas of the airfoil that affects its drag and performance characteristics of the airfoil are readily visible on the shape function curve as shown in the figure. Furthermore, the shape function provides easy control of the airfoil critical design parameters.

The term  $\sqrt{\psi} \bullet [1 - \psi]$  will be called the “Class Function”  $C(\psi)$  With the general form

$$C_{N2}^{N1}(\psi) = (\psi)^{N1} [1 - \psi]^{N2} \quad (6)$$

For a round nose airfoil  $N1 = 0.5$  and  $N2 = 1.0$

In reference 1, it was shown that different combinations of the exponents in the class function define a variety of basic general classes of geometric shapes:

- $C_{1.0}^{0.5}(\psi) \Rightarrow$  Defines a NACA type round nose and pointed aft end airfoil. (6.1)

- $C_{0.5}^{0.5}(\psi) \Rightarrow$  Defines a round nose / round aft end elliptic airfoil, or an ellipsoid body of revolution (6.2)

- $C_{1.0}^{1.0}(\psi) \Rightarrow$  Defines a biconvex airfoil pointed nose and pointed aft-end airfoil, or an ogive body. (6.3)

- $C_{0.75}^{0.75}(\psi) \Rightarrow$  Defines a Sears-Haack body which is the supersonic minimum wave drag body for a specified volume. (6.4)

- $C_{0.25}^{0.75}(\psi) \Rightarrow$  Defines a low drag projectile (6.5)

- $C_{0.001}^{1.0}(\psi) \Rightarrow$  Defines a cone or wedge airfoil. (6.6)

- $C_{0.001}^{0.001}(\psi) \Rightarrow$  Defines a rectangle, circular duct or circular rod. (6.7)

The “class function” is used to define general classes of geometries, where as the “shape function” is used to define specific shapes within the geometry class.

Defining an airfoil shape function and specifying it’s geometry class is equivalent to defining the actual airfoil coordinates which are obtained from the shape function and class function as:

$$\zeta(\psi) = C_{N2}^{N1}(\psi) \cdot S(\psi) + \psi \cdot \zeta_T \quad (7)$$

Reference 1 contains the shape functions for a variety of 2D airfoils and axi-symmetric bodies and nacelles.

## V. Representing the Shape Function

A number of different techniques of techniques of representing the shape function for describing various geometries will be described in this report. The simplest approach is illustrated in Figure 3. The figure shows the fundamental baseline airfoil geometry derived from the simplest of all shape functions, the unit shape function:  $S(\psi) = 1$ . Simple variations of the baseline airfoil are also shown with individual parametric changes of the leading edge radius, and of the trailing edge boat-tail angle.

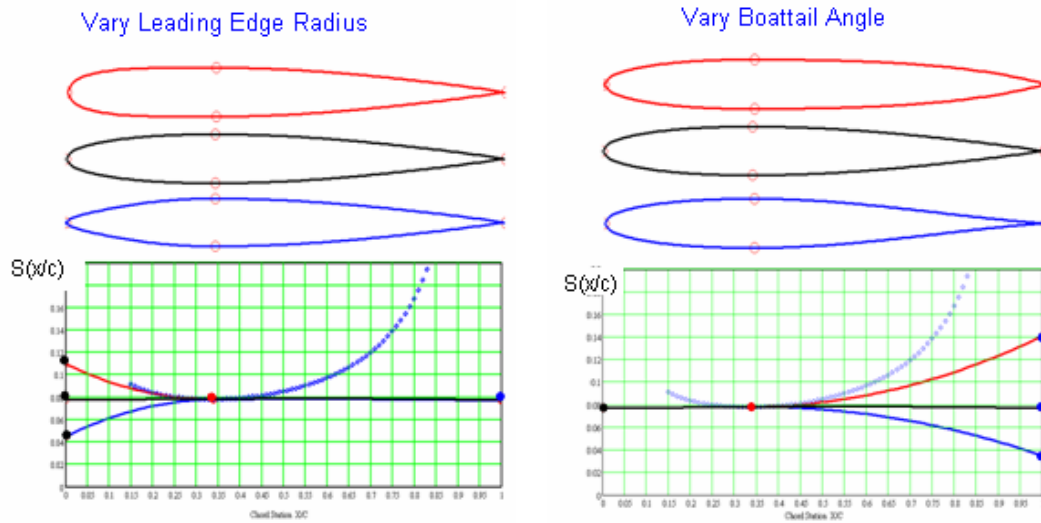


Figure 3: Examples of One Variable Airfoil Variations

The figure on the left shows changes in the leading edge radius and the front portion of the airfoil obtained by varying the value of  $S(0)$  with a quadratic equation that is tangent to the  $Z_{max}$  curve at  $x/c$  for  $Z_{max}$ . The maximum thickness, maximum thickness location and boat-tail angle remained constant.

The figure on the right shows variations in boat-tail angle obtained by changing the value of the shape factor at the aft end,  $x/c = 1$  while the front of the airfoil is unchanged. In each of these examples the airfoil shape changes are controlled by a single variable and in all cases the resulting airfoil is both smooth and continuous

Figure 4 shows a five variable definition of a symmetric  $C_{1.0}^{0.5}(\psi)$  airfoil using the shape function. The corresponding airfoil geometry is also shown. The variables include:

1. Leading edge radius
2. Maximum thickness
3. Location of maximum thickness
4. Boattail Angle
5. Closure Thickness

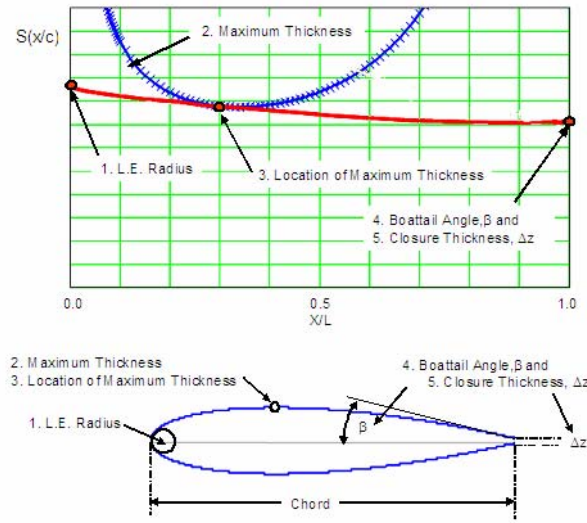


Figure 4: Symmetric Airfoil Five Variables Definition

A cambered airfoil can be defined by applying the same technique to both the upper and the lower surfaces. In this instance the magnitude of the value of the shape function at the nose,  $S(0)$ , of the upper and is equal to that on the lower surface. This insures that the leading edge radius is continuous from the upper to the lower surface of the airfoil. The value of the half thickness at the trailing edge is also equal for both surfaces. Consequently, as shown in figure 5, eight variables would be required to define the aforementioned set of parameters for a cambered airfoil.

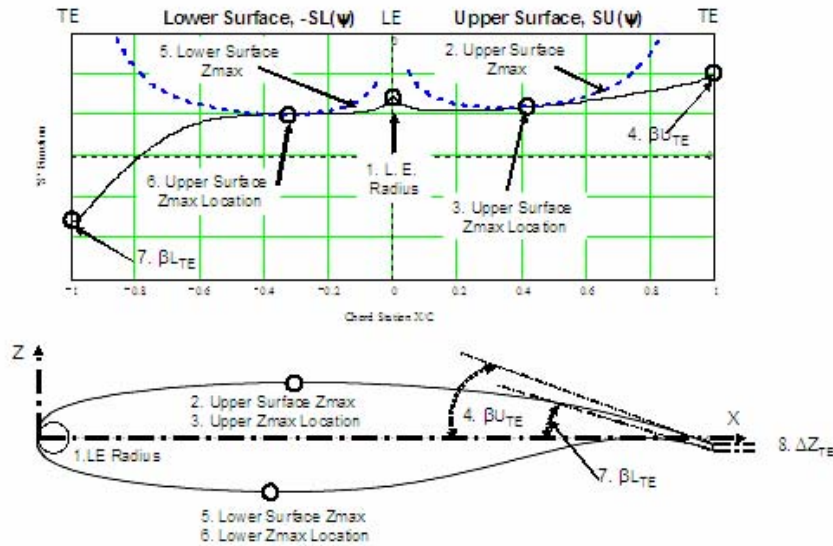


Figure 5: Cambered Airfoil Eight Variables Definition Definition

In the examples shown in figure 4 and figure 5, the key defining parameters for the airfoils are all easily controllable with the shape function.

## VI. Airfoil Decomposition into Component Shapes

In Figure 6, it is shown that the unit shape function defined by  $S(\psi) = 1$ , can be decomposed into two component shape functions

$S_1(\psi) = 1 - \psi$  which corresponds to an airfoil with a round nose and zero boat-tail angle

$S_2(\psi) = \psi$  which corresponds to an airfoil with zero nose radius and a finite boat-tail angle.



- "Sn(x)" Determines the Specific Geometry Shape

$$\zeta(\psi) = (\psi)^{N1} (1-\psi)^{N2} [S1(\psi) + S2(\psi)]$$

$$Sn(x/c) = S1(x/c) + S2(x/c)$$

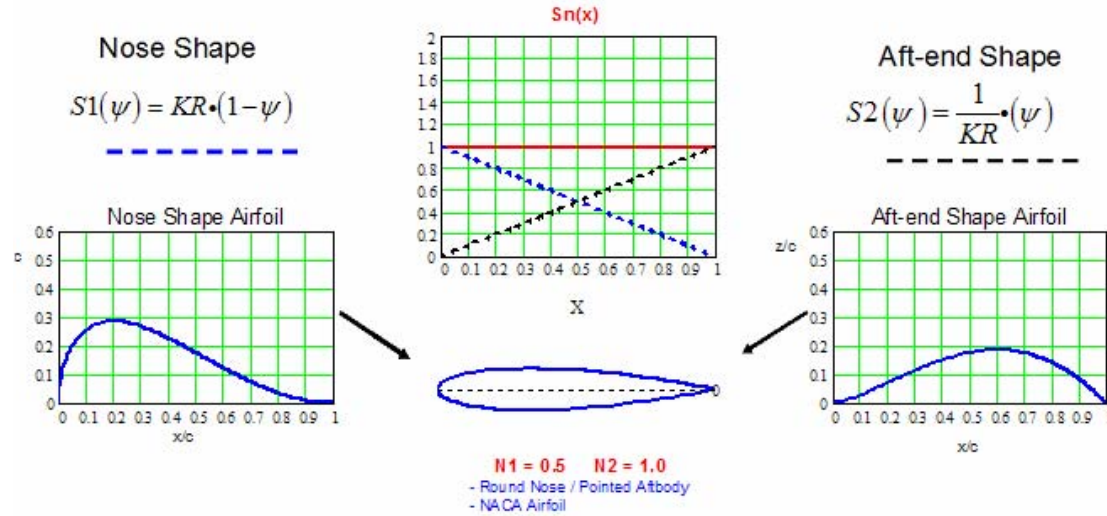


Figure 6: Airfoil Decomposition into Component Shapes or Basis Functions

An arbitrary scaling factor KR factor is shown in the figure as a weighting factor in the equations for the two component airfoils. By varying the scaling factor, KR, as shown in figure 7, the magnitudes of the leading edge radius and the boat-tail angle can be changed. This results in a family of airfoils of varying leading edge radius, boat-tail angle and location of maximum thickness.

- "Sn(x)" Determines the Specific Geometry Shape

$$\frac{z}{c} \left( \frac{x}{c} \right) = \left( \frac{x}{c} \right)^{N1} \left( 1 - \frac{x}{c} \right)^{N2} [S1\left(\frac{x}{c}\right) + S2\left(\frac{x}{c}\right)]$$

$$Sn(x/c) = S1(x/c) + S2(x/c)$$

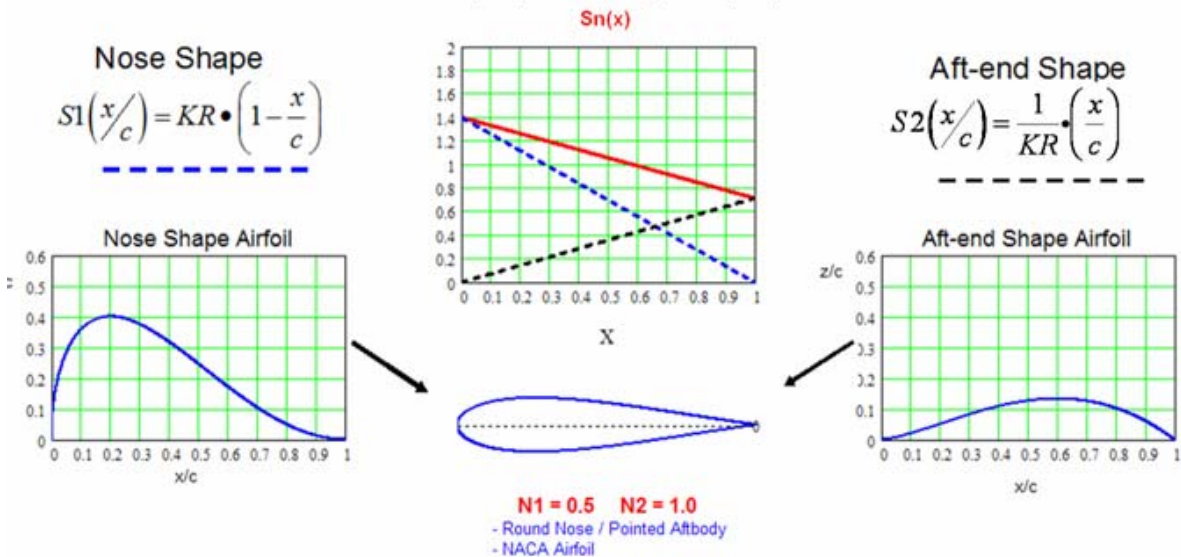


Figure 7: Airfoil Geometry Change by Varying Component Shape Functions

The unit shape function can be further decomposed into component airfoils by representing the shape function with a Bernstein polynomial of order “N” as shown in figure 8.

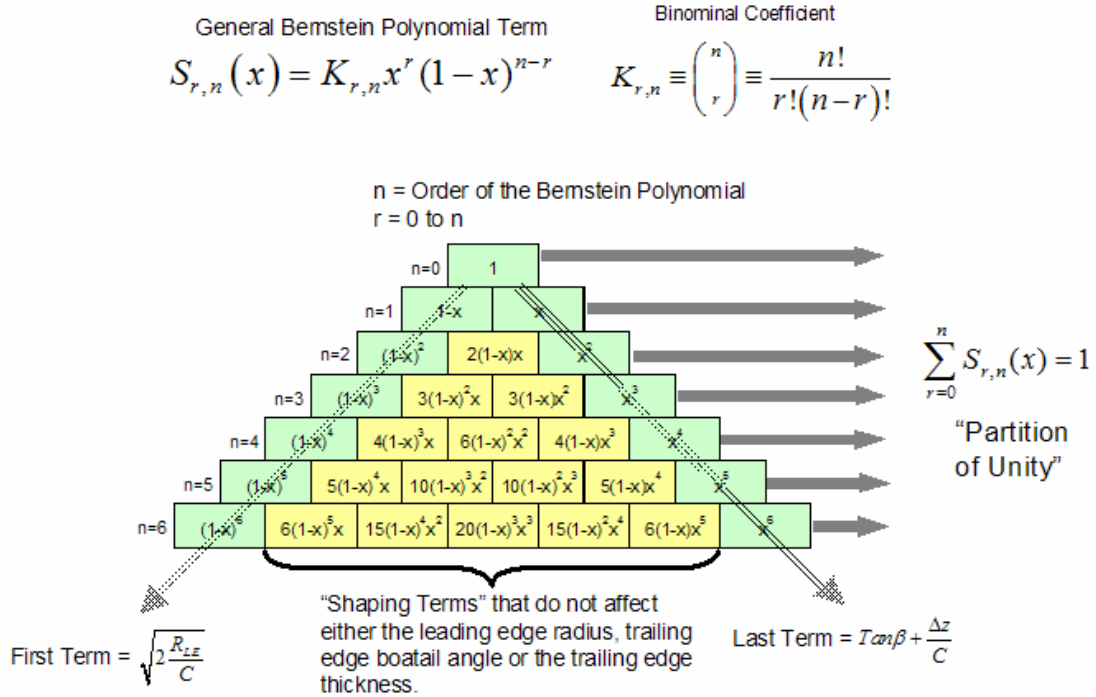


Figure 8: Bernstein Polynomial Decomposition of the Unit Shape Function

The representation of the unit shape function in terms of increasing orders of the Bernstein polynomials provides a systematic decomposition of the unit shape function into scaleable components. This is the direct result of the “Partition of Unity” property which states that the sum of the terms, which make up a Bernstein polynomial of any order, is equal to one. This means that every Bernstein polynomial represents the unit shape function. Consequently, the individual terms in the polynomial can be scaled to define an extensive variety of airfoil geometries.

The Bernstein polynomial of any order “n” is composed of the “n+1” terms of the form:

$$S_{r,n}(x) = K_{r,n} x^r (1-x)^{n-r} \quad (8)$$

r = 0 to n

n = order of the Bernstein polynomial

In the above equation, the coefficients factors  $K_{r,n}$  are binominal coefficients defined as:

$$K_{r,n} \equiv \binom{n}{r} \equiv \frac{n!}{r!(n-r)!} \quad (9)$$

For any order of Bernstein polynomial selected to represent the unit shape function, only the first term defines the leading edge radius and only the last term defines the boat-tail angle. The other in-between terms are “shaping terms” that neither affect the leading edge radius nor the trailing edge boat-tail angle.

Examples of decompositions of the unit shape function using various orders of Bernstein polynomials are shown in figure 9 along with the corresponding component airfoils.

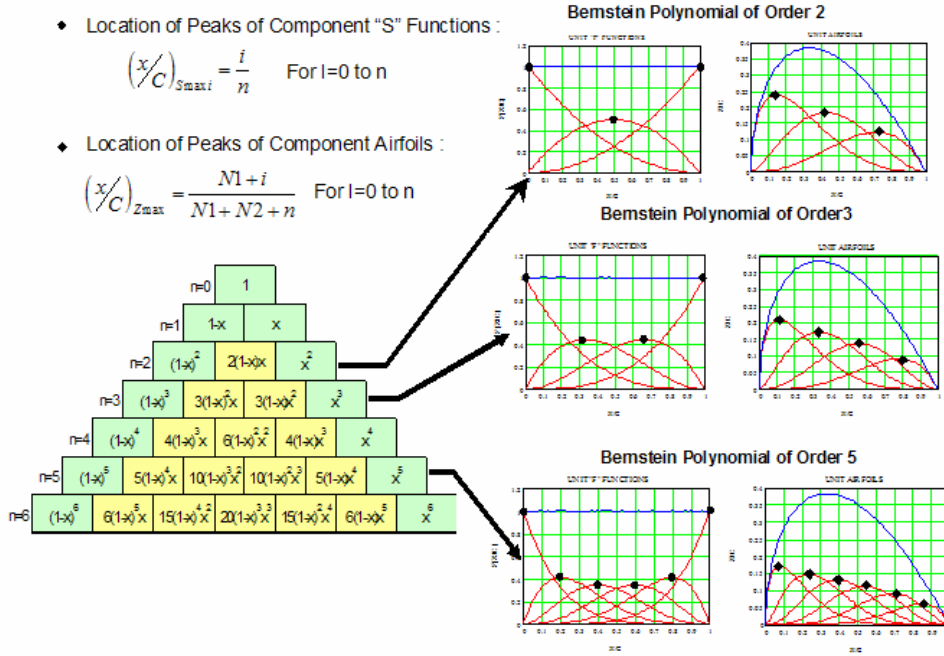


Figure 9: Bernstein Polynomial Provides “Natural Shapes”

The locations of the peaks of the component “S” functions are equally spaced along the chord as defined by the equation:

$$\left(\psi\right)_{S_{\max i}} = \frac{i}{n} \quad \text{for } i = 0 \text{ to } n \quad (10)$$

The corresponding locations of the peaks of the component airfoils are also equally spaced along the chord of the airfoil and are defined in terms of the class function exponents and the order of the Bernstein polynomial by the equation:

$$\left(\psi\right)_{Z_{\max}} = \frac{N1+i}{N1+N2+n} \quad \text{for } i = 0 \text{ to } n \quad (11)$$

The technique of using Bernstein polynomials to represent the shape function of an airfoil in reality defines a systematic set of component airfoil shapes that can be scaled to represent a variety of airfoil geometries.

## VII. Airfoils Defined Using Bernstein Polynomials Representation of the Unit Shape Function

The upper and lower surfaces of a cambered airfoil, can each be defined using Bernstein Polynomials of any selected order  $n$ , to describe a set of component shape functions that are scaled by “to be determined” coefficients as shown in the following equations.

The component shape functions are defined as:  $S_i(\psi) = K_i \psi^i (1-\psi)^{n-i}$  (12)

Where the term  $K_i$  is the binomial coefficient which is defined as:  $K_i \equiv \binom{n}{i} = \frac{n!}{i!(n-i)!}$  (13)

Let the trailing edge thickness ratios for the upper and lower surface of an airfoil be defined as:

$$\Delta \xi_U = \frac{z_{u_{TE}}}{C} \quad \text{and} \quad \Delta \xi_L = \frac{z_{l_{TE}}}{C} \quad (14)$$

The class function for the airfoil is:  $C_{N2}^{N1}(\psi) = \psi^{N1} \cdot (1 - \psi)^{N2}$  (15)

The overall shape function equation for the upper surface is:  $Su(\psi) = \sum_{i=1}^n Au_i \cdot S_i(\psi)$  (16)

The upper surface defining equation is:  $(\zeta)_{Upper} = C_{N2}^{N1}(\psi) \cdot Sl(\psi) + \psi \cdot \Delta \xi_{Upper}$  (17)

The lower surface is similarly defined by the equations:  $Sl(\psi) = \sum_{i=1}^n Al_i \cdot S_i(\psi)$  (18)

and  $(\zeta)_{Lower} = C_{N2}^{N1}(\psi) \cdot Sl(\psi) + \psi \cdot \Delta \xi_{Lower}$  (19)

The coefficients  $Au_i$  and  $Al_i$  can be determined by a variety of techniques depending on the objective of the particular study. Some examples include:

- Variables in a numerical design optimization application
- Least squares fit to match a specified geometry
- Parametric shape variations.

The method of utilizing Bernstein polynomials to represent an airfoil has the following unique and very powerful properties<sup>1</sup>:

- This airfoil representation technique, captures the entire design space of smooth airfoils
- Every airfoil in the entire design space can be derived from the unit shape function airfoil
- Every airfoil in the design space is therefore derivable from every other airfoil

## VIII. Example Airfoil Representation – RAE2822

An example of the ability of the class function / shape function methodology to represent a typical supercritical airfoil, RAE2822, with increasing orders of Bernstein polynomials is shown in figures 10 through 13.

The airfoil geometry as “officially” defined by 130 “x,z” coordinates is shown in Figure 10. The shape functions for the upper and lower surface, as calculated from these coordinates, are also shown. The shape function curves are seen to be very “simple” curves as compared to the actual airfoil upper and lower surfaces.

Shape functions calculated by the method of least squares to match the defining coordinates and corresponding to increasing orders of Bernstein's polynomials, are compared with the shape function determined from the actual RAE2822 geometry coordinates figure 11. The corresponding airfoil geometry representation is shown in figure 12. The locations of the peaks of the component shape functions and the corresponding component airfoils and are indicated in the individual figures.

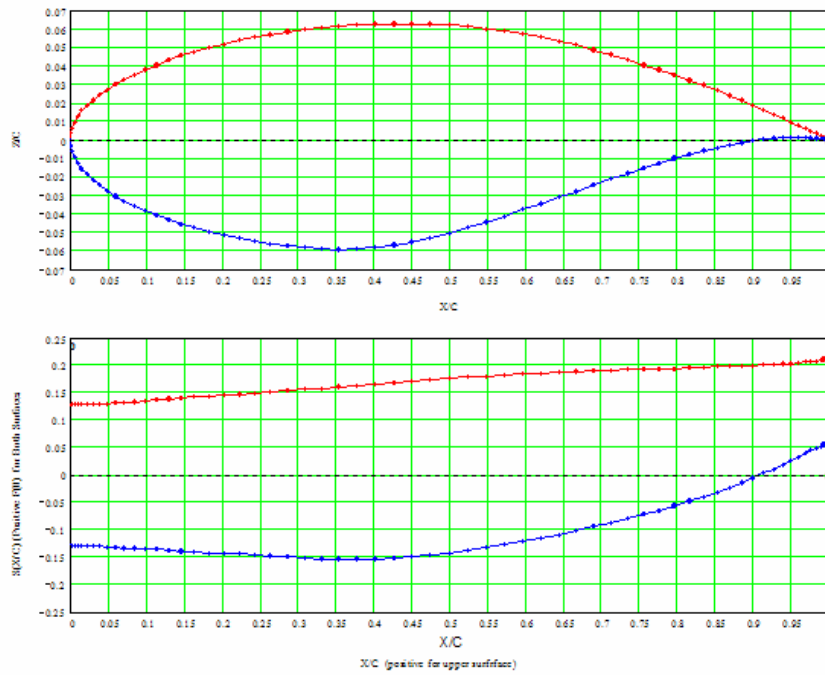


Figure 10: RAE 2822 Airfoil Geometry – (Defined by 130 “X, Z” Coordinates)

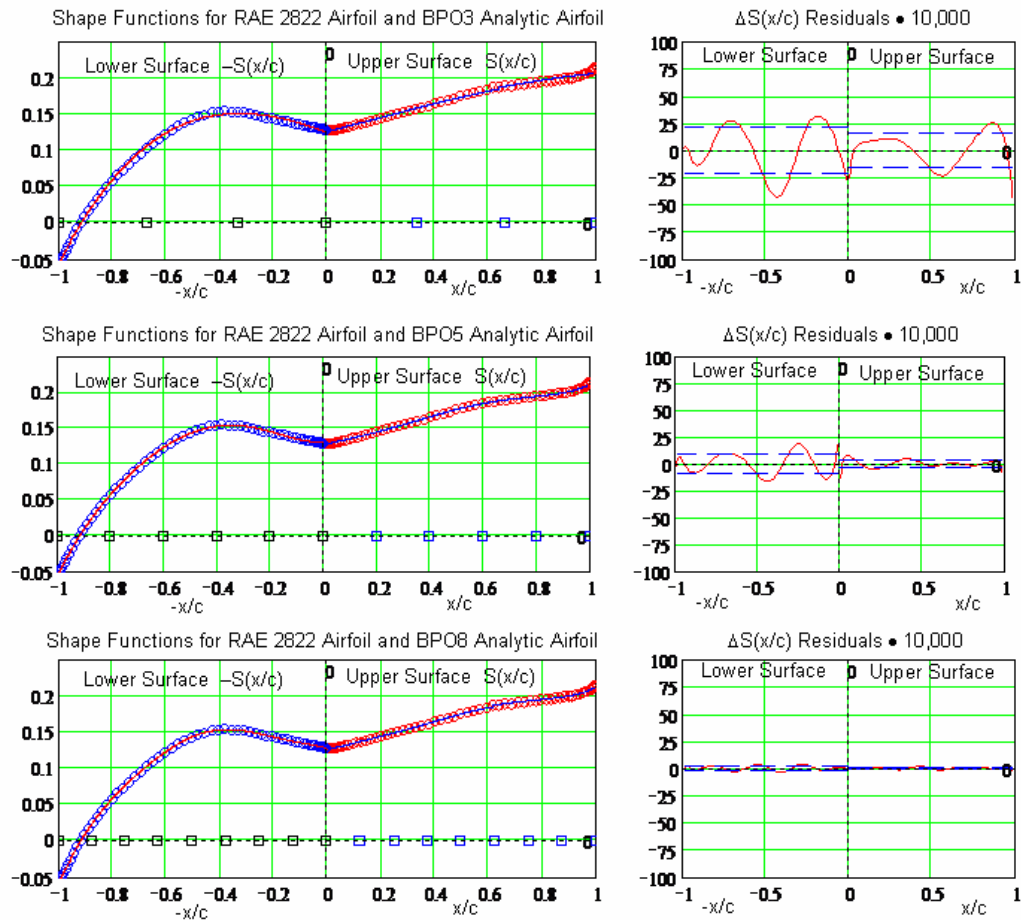


Figure 11: RAE2822 Shape Function Convergence Study

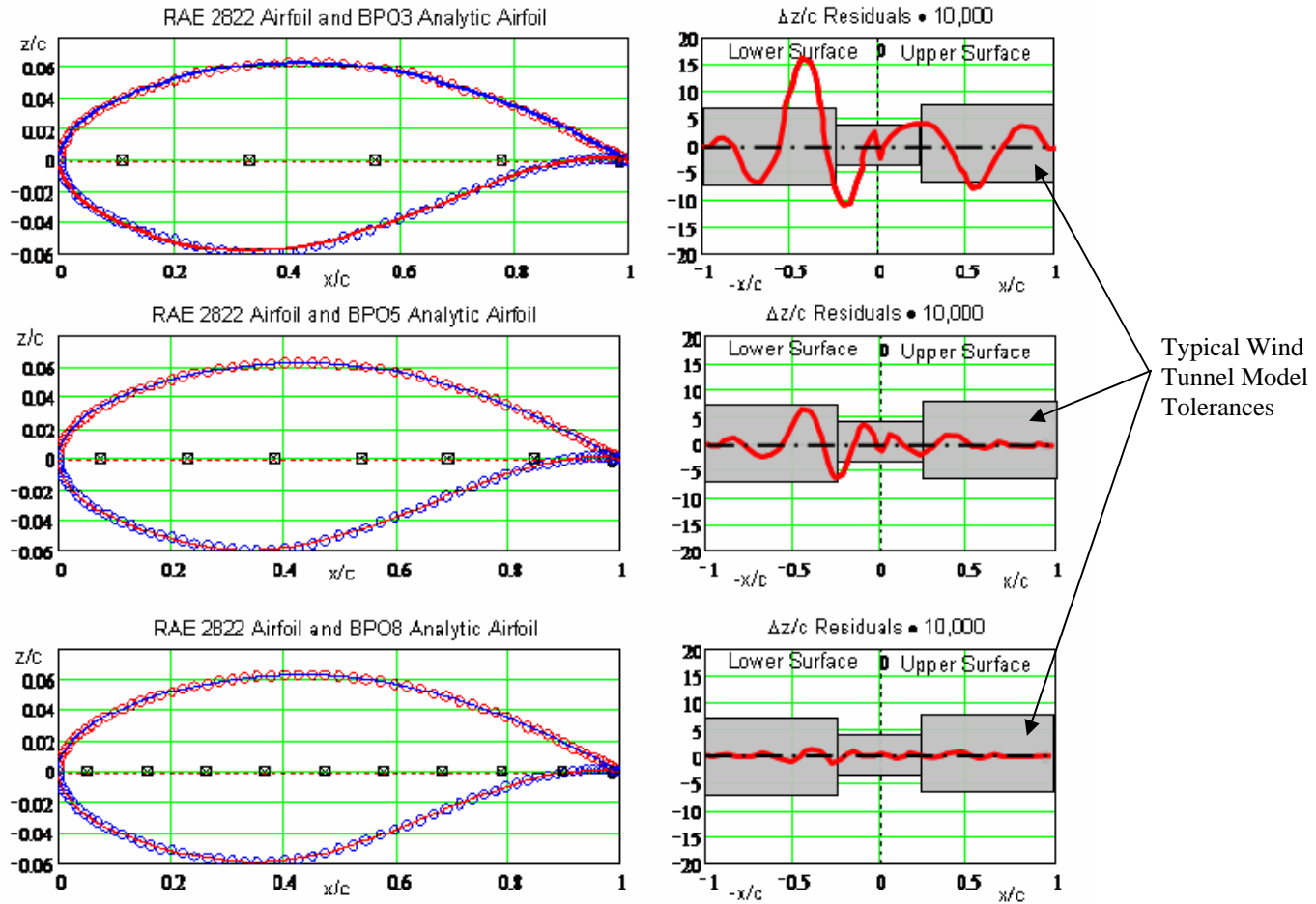


Figure 12: RAE2822 Geometry Convergence Study

The residual differences between shape function residuals, and the surface coordinate residuals are also shown in the figures. The differences between the actual and the approximated shape functions and surface coordinates are hardly discernible even for the Bernstein polynomial of order 3, BPO3, representation. The oscillating nature of the residual curves is typical of any least squares fit.

The results obtained with BPO5 and PBO8 show that the residual differences rapidly and uniformly vanish with increasing order of the representing Bernstein polynomial. The differences between the BPO5 and BPO8 approximate airfoils and the actual geometry are well within typical wind tunnel model tolerances.

Corresponding detailed comparisons of the surface slopes, second derivatives and surface curvature are also shown in reference 1. Calculations of surface pressure distributions between the actual and represented geometries were also made using the TRANAIR<sup>3</sup> full potential CFD code with coupled boundary layer. The lift predictions for all BPO5 and greater airfoils matched the RAE 2822 predictions. The drag predictions and pressure distributions for BPO8 and above agreed exactly with the RAE 2822 predictions.

Similar results were also shown in reference 1 for a number of other airfoil geometries. The results of the geometry, CP and force comparisons implied that a relatively low order BP shape function airfoil with only a relatively small number of variables can closely represent any airfoil<sup>1</sup>.

The mathematical simplicity the shape function representation of an airfoil is clearly evident in figure 13. In this figure the surfaces slopes, 2<sup>nd</sup> derivatives and surface curvature for the airfoil surfaces are compared with the corresponding values for the airfoil as defined by a shape function defined airfoil representation.

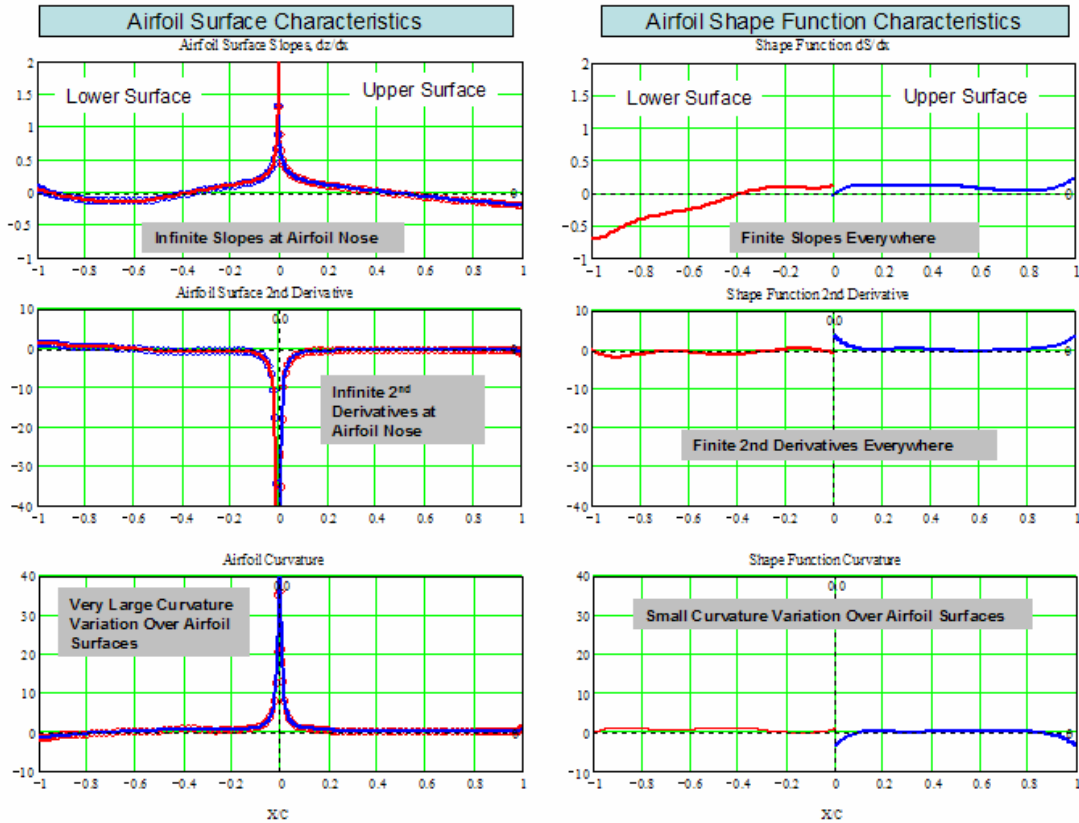


Figure 13: Mathematical Simplicity of the Shape Function – RAE 2822

The slopes and second derivatives of the RAE2822 airfoil are infinite at the nose, and the curvature varies greatly over the surface of the airfoil. The slopes and 2nd derivatives are finite, and everywhere small for the RAE2822 shape function, and the curvature of the shape function is essentially zero. This clearly shows the distinct advantage of mathematical simplicity that the shape function airfoil representation methodology has relative to the use of the actual coordinates of the airfoil.

The results of the previously reported extensive investigations<sup>1</sup> of the adequacy of the shape function methodology utilizing Bernstein polynomials to represent a wide variety of airfoils, showed that a relatively low order Bernstein polynomial, (typically BPO6 to BPO9), matched the airfoils geometries, slopes and 2<sup>nd</sup> derivatives as well as the pressure distributions and aerodynamic forces<sup>1</sup>. The results also indicated that lower order Bernstein polynomials, corresponding to fewer design variables, (perhaps BPO4 to BPO6), should be adequate for developing optimum designs.

The methodology offers the option for a systematic approach for design optimization. The optimization process can initially be conducted with a family of component airfoil shapes corresponding to a low order BP representation for the shape function to obtain an optimum design. The order of the BP can then be increased to conduct another optimization to determine if a better optimum design is achieved. Increasing the order of the BP is a systematic way to increase the number of design variables and thereby explore the convergence of an optimum solution.

The discussions so far have been focused in 2D round nose / sharp aft-end airfoils. However, as shown in figure 14, different combinations of the exponents in the class function defines a variety of basic general classes of geometric shapes of airfoils, bodies of revolution and axi-symmetric nacelles.



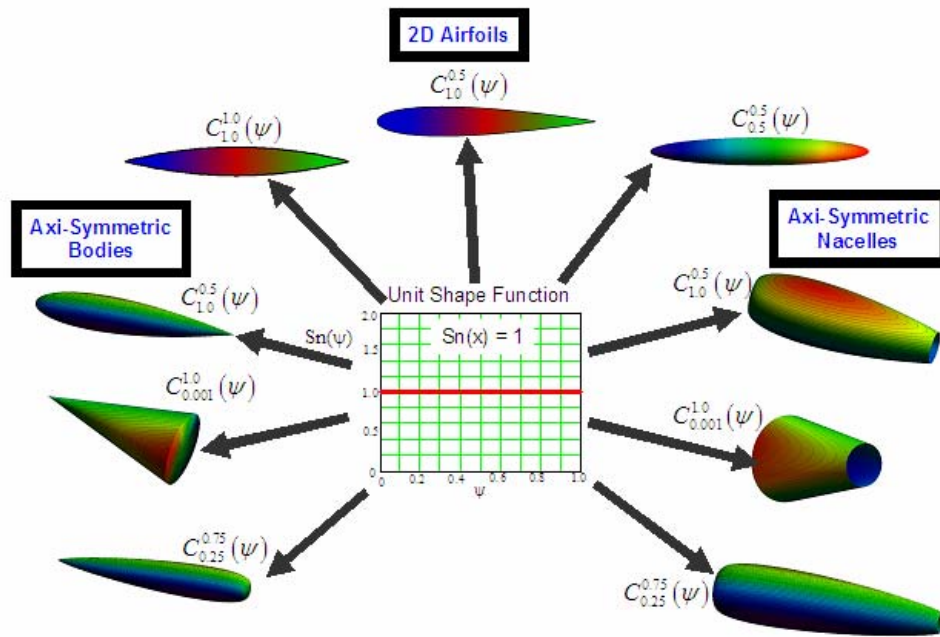


Figure 14: Geometries Derivable From a Unit Shape Function

The use of the class function therefore, allows the previously discussed shape function methodology as well as the studies conclusions to apply equally well to a wide variety of 2D and axis-symmetric geometries.

## IX. Extension to Arbitrary 3D Geometries

The shape function / class function methodology of representing a 2D or axis-symmetric geometry will now be shown to be directly applicable for representation of the cross sectional shapes of the class 2 aerodynamic components which are the “body type” geometries.

Let us initially assume that a body cross-section is laterally symmetric and has the shape of an ellipse as shown in the figure 15.

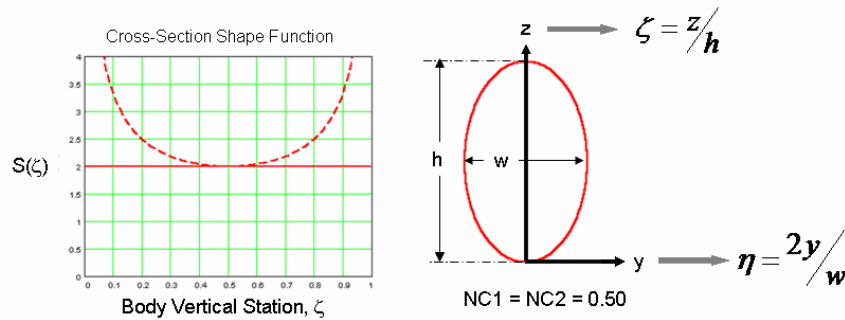


Figure 15: Shape Function / Class Function Representation of a Body Cross Section

We will then subsequently generalize the results using the class function to other cross-sectional geometries.

The equation for an ellipse as shown in the figure is:

$$\left(\frac{2Y}{w}\right)^2 + \left(\frac{2Z-h}{h}\right)^2 = 1$$



Let  $\eta = 2y/w$  and  $\zeta = z/h$

The ellipse equation becomes:  $\eta^2 + (2\zeta - 1)^2 = 1$  or  $\eta = 2\sqrt{\zeta} \cdot \sqrt{1-\zeta}$

The cross-section can there be expressed in terms the class function and shape function as:

$$\eta = S(\zeta) \cdot C_{0.5}^{0.5}(\zeta)$$

The cross section shape function is simply a constant:  $S(\eta) = 2$ . The opposing side is defined by the condition of lateral symmetry. As Shown in figure 16, varying the exponents of the class function can provide a wide variety of body cross section shapes.

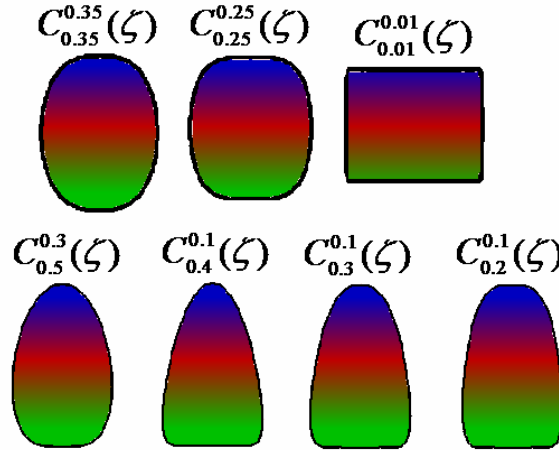


Figure 16: Various Body Cross-sectional shapes

Another method to describe the cross sectional of a body is to use the shape functions to describe the upper and the lower lobes of a body cross section each as shown in figure 17

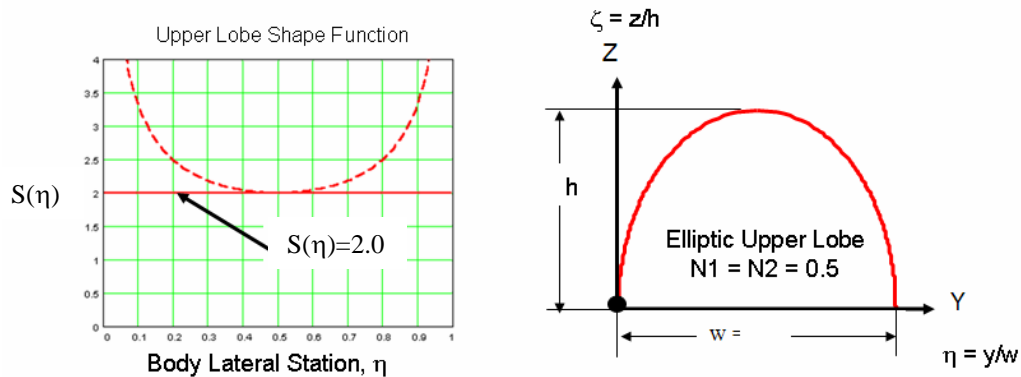


Figure 17: Representation of a Body Upper or Lower Lobe Shape

In this case the upper lobe defining equation is:  $\zeta u(\eta) = [Su(\eta) \equiv 2] \cdot Cu_{0.5}^{0.5}(\eta)$

Figure 18 shows examples of variety of cross section shapes that can be obtained by independently varying the class function coefficients for the upper and lower lobes of the body cross section.

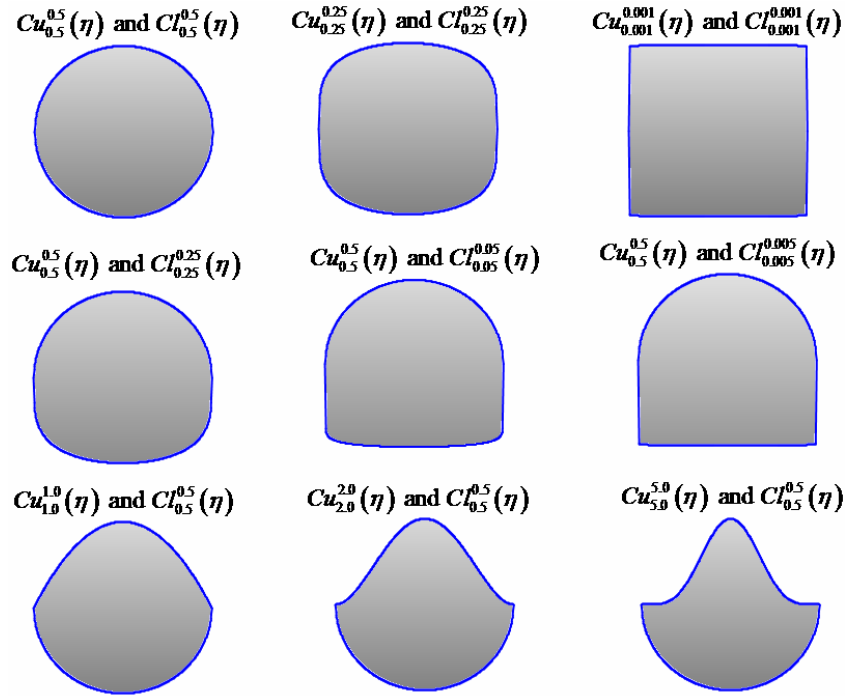


Figure 18: Example Upper Lobe / Lower Lobe Body Cross sections

The example cross-sections shown in figures 17 and 18 were obtained using simple unit shape functions but different class functions. Very general cross-sectional shapes can be generated by varying the shape function formulations in addition to the class functions. As shown in figure 19, changing the shape function for the upper body lobe can create upper surface bumps or fairings. In the examples shown, the geometries are representative of a cross-section of a fuselage through the cockpit area.

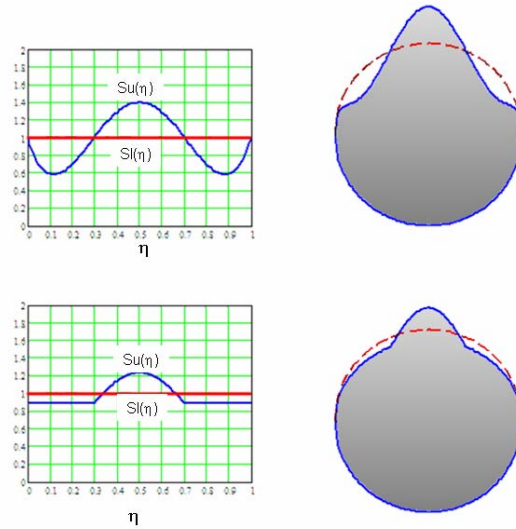


Figure 19: Fuselage "Bump" Representation

Three dimensional bodies in general can be represented as a cross-sectional shape together with a distribution of the cross-section shapes. This is shown in figure 20 by the examples of a duct, a high aspect ratio wing, and a supersonic type integrated wing body.

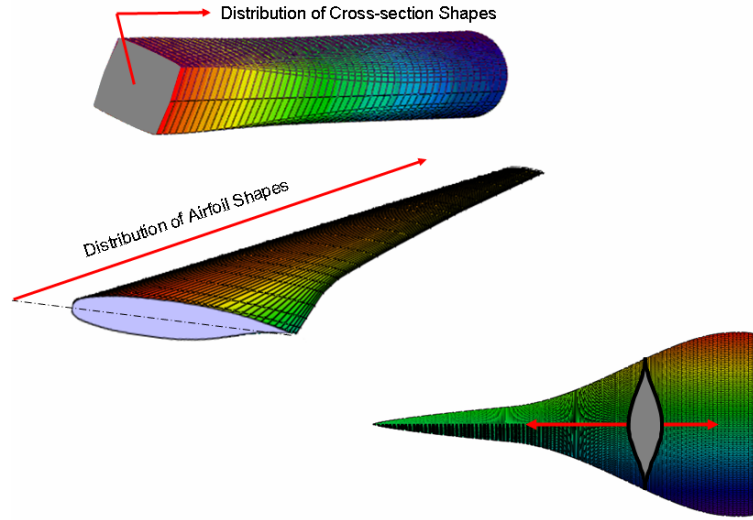


Figure 20: Examples of 3D Geometries as Distribution of Shapes

The concept of using the shape function / class function methodology to describe both the fundamental cross-sectional shapes and the distribution of the shapes along the body axis is shown for the simple case of a cube in figure 21.

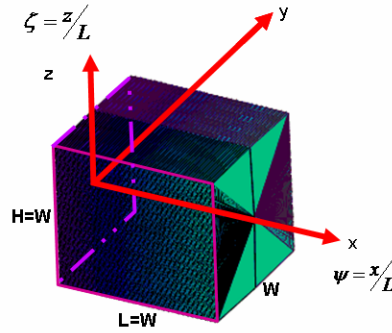


Figure 21: Definitions of Cross-Section Shape and Distribution

The square cross-section can be described by a class function with “zero exponents”,  $Cs_{0.005}^{0.005}(\eta)$ , and a unit shape function. The longitudinal area distribution controls the distribution of the cross section shapes. The longitudinal area distribution for a cube can be represented by a similar class function,  $Cd_{0.005}^{0.005}(\psi)$

Figure 22 shows an example of using the shape function / class function methodology to make an apparently significant geometry changes with very few design variables, by transforming a cube into an equal volume Sears-Haack body.

The circular cross-section of the Sears-Haack body has unit shape function and class functions exponents equal to  $Cs_{0.5}^{0.5}(\eta)$ . The longitudinal radius distribution of a Sears-Haack body has a unit shape function and a class function equal to  $Cd_{0.75}^{0.75}(\psi)$ .

Consequently the transformation of the cube into a Sears-Haack body is easily obtained by simultaneous:

- Increasing the cross-section class function exponents from 0.005 to 0.5
- Increasing the longitudinal radius distribution class function exponents from 0.005 to 0.75
- Increasing the length to keep the volume constant.

Figure 22 shows a number of intermediate geometries as the cube is transformed into the Sears-Haack body.

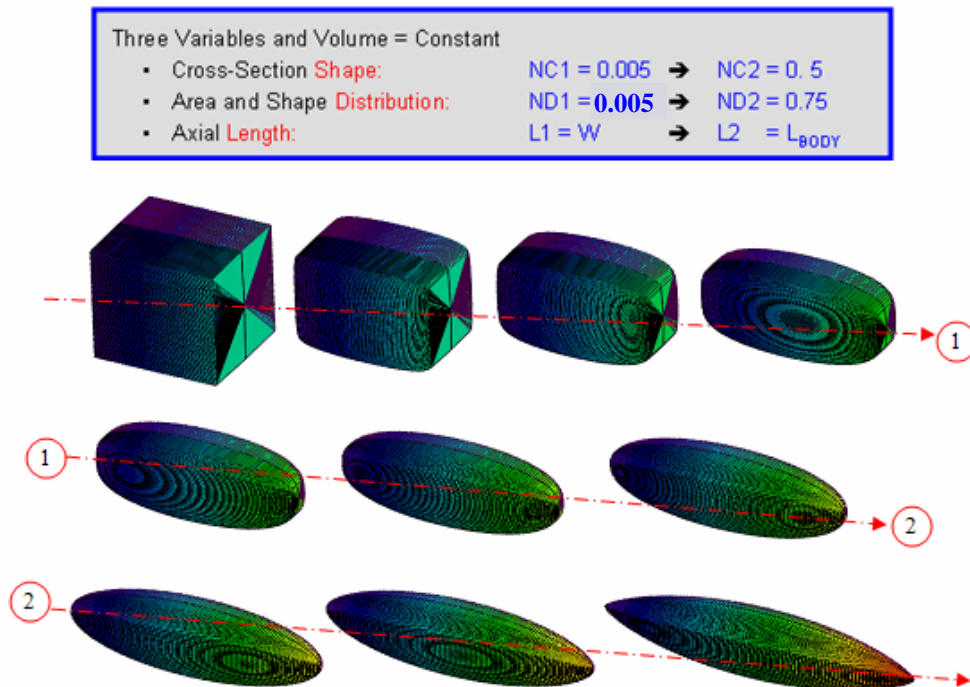


Figure 22: Three Variable Transformation of a Cube into a Sears-Haack Body

An example of transforming a constant area circular duct into a circular duct with geometry that varies from a circular inlet to a square shaped nozzle, can be easily defined using is variable class function exponents as shown in figure 23.

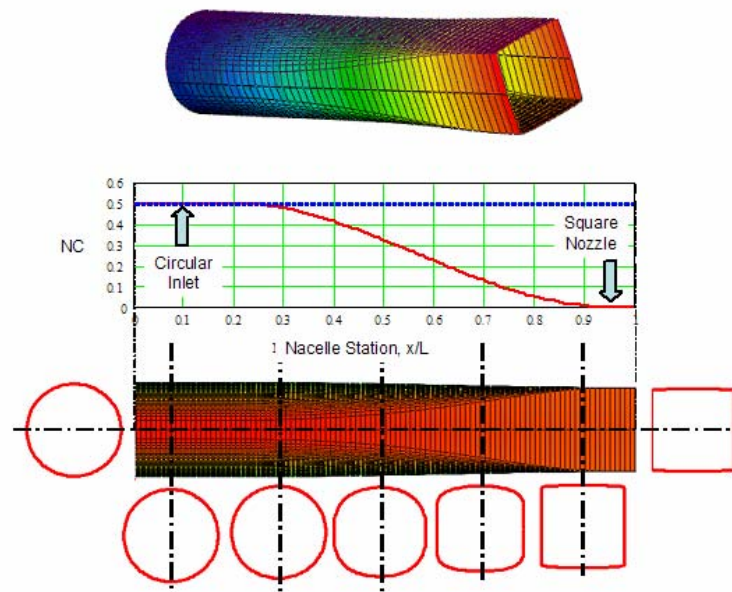


Figure 23: One Variable Definition of a Circular Duct With a Square Nozzle

The initial geometry shape at the inlet is a circular duct defined with a cross-section class function with exponents equal to “0.5”. The duct geometry, in this example, retains a constant cross section from 0 to 20% of the length. The last 5% length of the duct has a square cross-section which has class function exponents equal to “0.005”. The width/ depth of the square were sized to match the circular inlet area.

In between 20% and 95% of the length, the class function exponents were decreased from 0.5 at 20% to 0.005 at 95% by a cubic variation with zero slopes at both ends. Along the transition region the width and depth were scaled proportionally to keep the cross section area constant. The entire geometry is in reality driven by a single variable, the aft end constant class function exponent

This is an example of a “scalar” or “analytic” loft in which the geometry is generated by the analytic variation of the shape parameters along the length of the duct.

Figure 24 shows two 3D bodies that are defined by a total of 5 parameters:

- The geometric shape is defined by the cross-section class function and the area distribution class function.
- The body size is defined by three length parameters which include the overall length, width and height

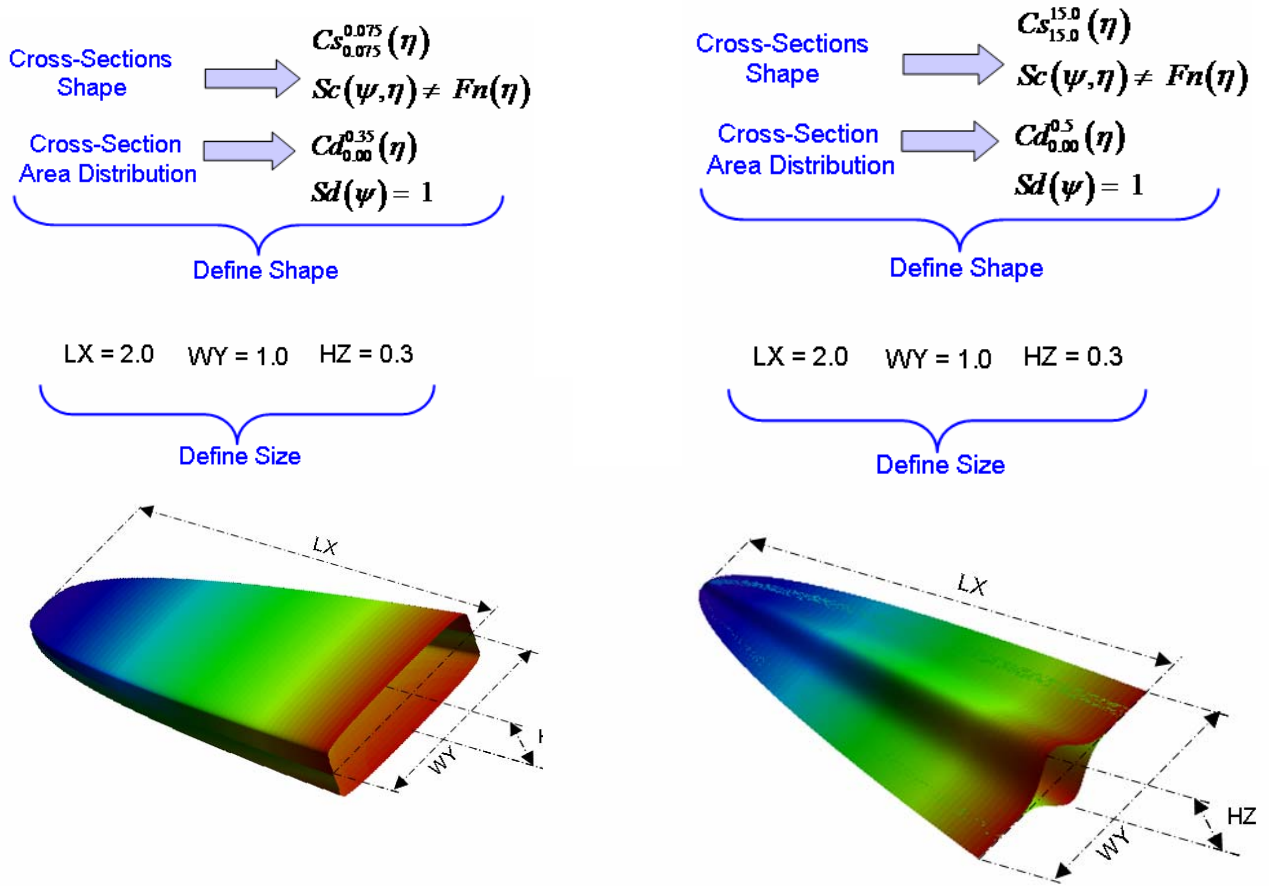
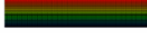
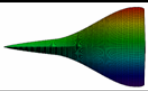


Figure 24: Simple 3D body Examples Defined by 2 Class Functions and 3 Size Parameters

In figure 25, using a similar technique to that used to define the duct in figure 23, a circular duct is transformed a geometric shape that appears very similar to a supersonic aircraft configuration.

PARAMETER		
LENGTH, L	10	100
L/Dmax	5	5
$Cs_{NC}^{NC}(\eta)$	Nc = 0.5	Nc( $\psi$ ) [Figure A]
$e = W/H$	1.0	$\varepsilon(\psi)$ [Figure B]
STATION 1		0.35
STATION 2		0.9
$Cd_{Nd1}^{Nd1}(\eta)$	Nd1 = 0.0 Nd2 = 0.0	Nd1 = 0.75 Nd2 = 0.005

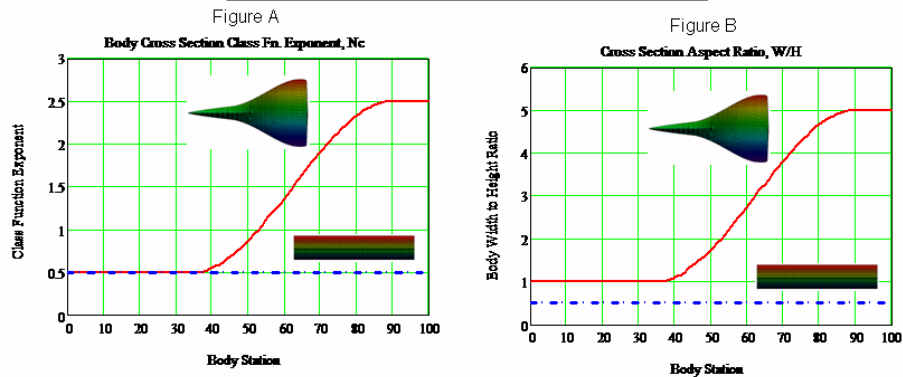


Figure 25: Transformation of a Circular Cylinder in a “Supersonic Transport”

This geometric transformation was obtained with a total of four design variables. The four design variables included:

- Longitudinal class function exponents: Nd1, Nd2
- Aft end cross-section class function exponent, NC,
- the width to height ratio at the aft end: e2

Figure 26 shows a series of cross-section cuts through the final configuration to illustrate the smoothness of the geometry transition.

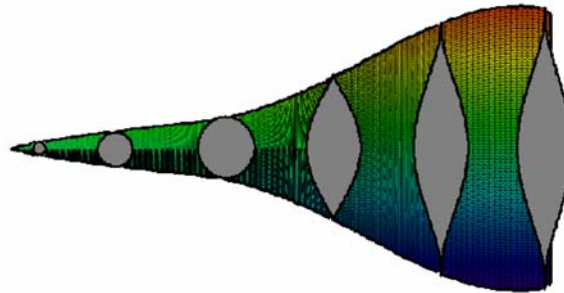


Figure 26: wing / Body Cross-Section Cuts

## X. Nacelle Design – 2 Options

There are two options for using class functions and shape functions for defining a nacelle. These include

1. Define Longitudinal profile shapes for crown line, maximum half-breadth, and keel line and then distributing these profiles circumferentially around the longitudinal axis to define the nacelle geometry
2. Define cross section shapes and distribute the shapes along the longitudinal axis as controlled by an area distribution.

In the discussions that follow, we will focus on the 1st option, since this will provide a demonstration of the combined use of many of the concepts that have been shown in this report and in the previous studies<sup>1</sup>. The objective is to develop a detailed nacelle definition with the use of very few design variables.

Figure 27 shows the common approach to defining a nacelle using airfoil type sections for the crown line, keel line and maximum half breadth shapes. In the example, the basic airfoil geometries are represented by a BP5 shape function definition for a supercritical type airfoil which therefore has 6 defining variables.

The keel line airfoil and the max half breadth airfoils in this example are both parametrically modified forward of the maximum thickness station to increase the leading edge radius in the former case and decrease the leading edge radius in the latter case. This results in the addition of two more defining variables corresponding to the desired leading edge radii.

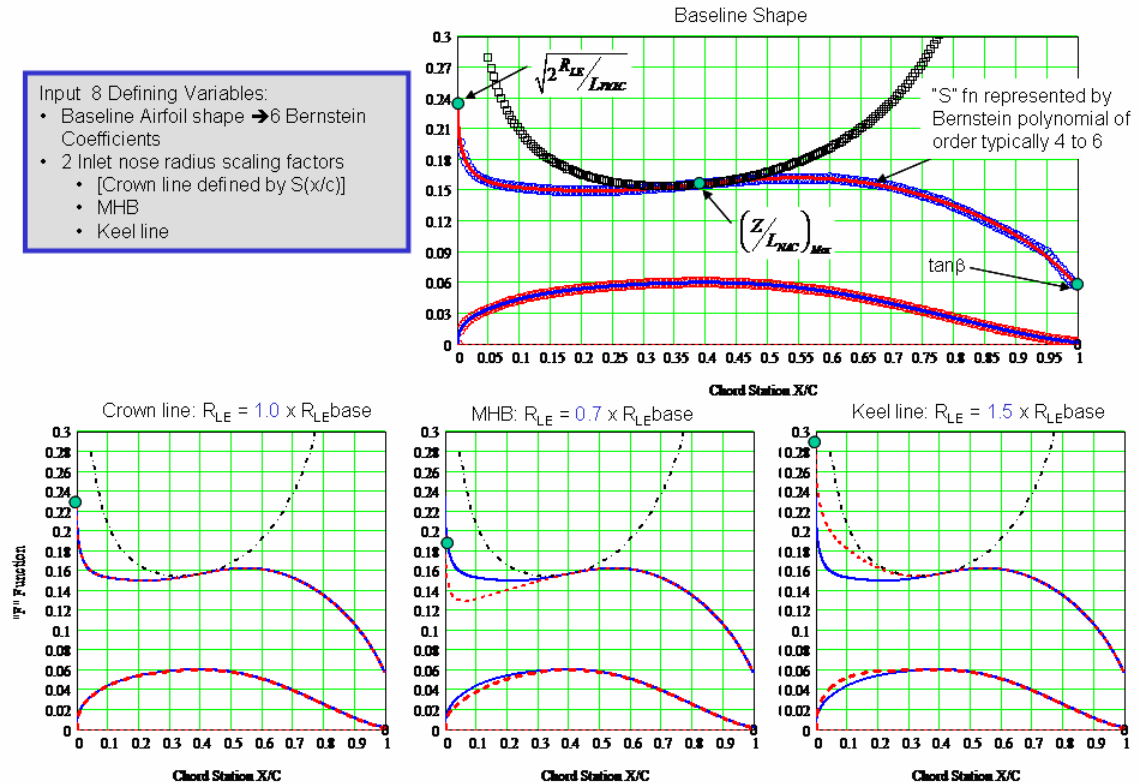


Figure 27: Nacelle Crown Line, Keel Line and Max Half Breadth Definitions  $\rightarrow$  8 Variables

The external cross-sectional shape of the nacelle between the crown, max half breadth and keel is defined by an upper lobe class function with the exponent NU. The lower lobe of the nacelle is similarly defined by lower lobe class function with the exponent NL. This approach to distribute the longitudinal airfoil shapes circumferentially around the nacelle is shown in figure 28. This is achieved by the use of cross section class functions in which the class function exponents are varied along the length of the nacelle as shown in the figure.

The upper lobe for the entire nacelle is defined using a constant class function exponents of 0.5. This results in an elliptic / circular cross sectional shape distribution between the crown line and the maximum half breadth airfoils.

The lower lobe cross-section class function exponents equal 0.25 out to defining station 1 which is located at 40% of the nacelle length. This results in a “squashed” shape distribution from the maximum half breadth airfoil to the keel line airfoil over the front portion of the nacelle.

The lower lobe aft of defining station 2, which occurs at 80% of the nacelle length, is circular with a class function exponent equal to 0.5. Consequently this results in an axi-symmetric nozzle geometry.



In between station 1 and station 2, the lower lobe shape joining the maximum half breath geometry and the keel geometry, varies smoothly from a squashed section at station 1 to a circular section at station 2.

The cross-sectional shape distribution is therefore defined entirely by the following 4 design variables:

- Upper lobe class function exponents, NU
- Lower lobe Class Functions, NL
- End of squashed lower lobe station, Station 1
- Start of circular lower lobe station, Station 2

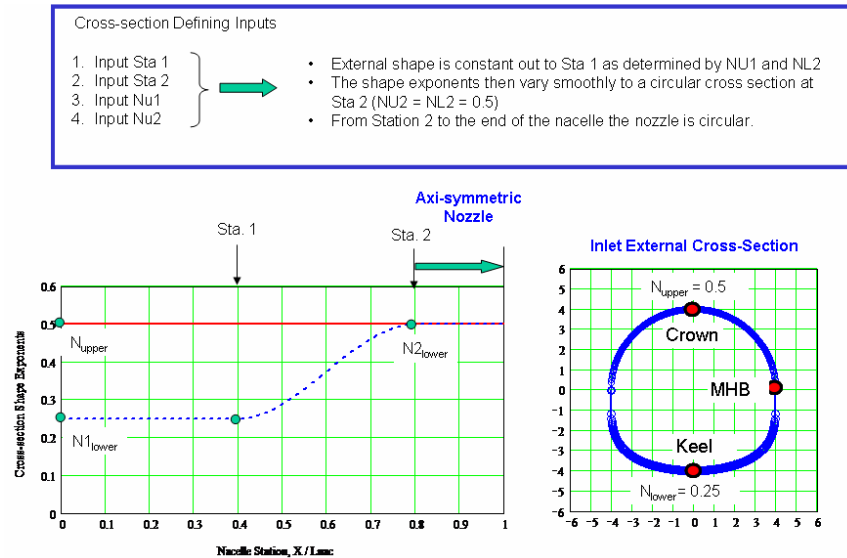


Figure 28: Nacelle Shape Distribution Circumferentially Around the Nacelle Centerline → 4 Variables

The inlet definition is shown in figure 29. The internal inlet cross-section shape and leading edge radii distribution were defined to match the external cowl cross-section shape and streamwise leading edge radius distribution at the nose of the nacelle.

The internal inlet shape then varied smoothly from the “squashed” shape at inlet lip to a circular cross-section at the throat station. The internal shape was defined as circular aft of the throat station to the end of the inlet length.

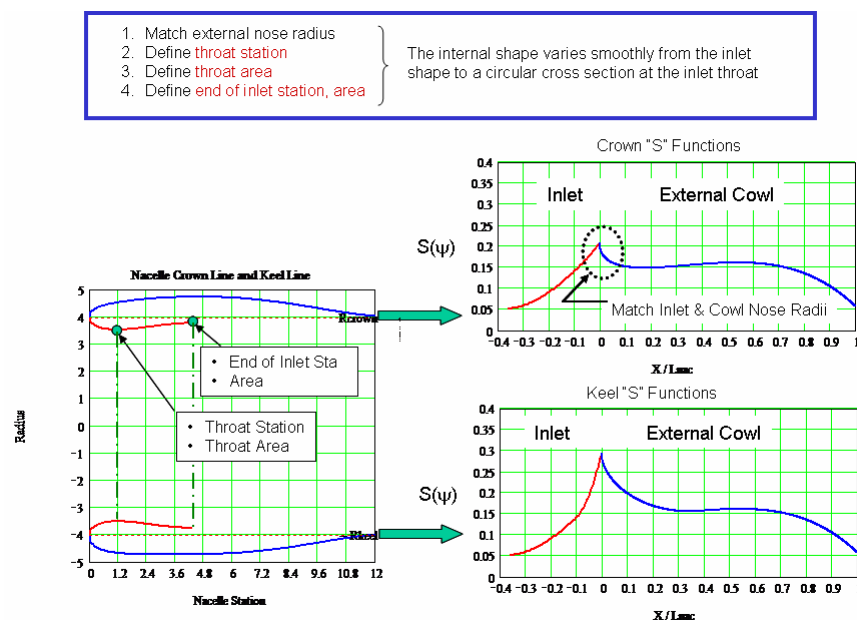


Figure 29: Nacelle Inlet Geometry Definition → 4 variables



The entire internal inlet geometry required only 4 more defining variables. These include:

- Throat Station
- Throat Area
- End of Inlet station
- End of Inlet area

The complete nacelle geometry as defined by the aforementioned 15 total nacelle design variables is shown in figure 30. The geometry is seen to be everywhere smooth and continuous.

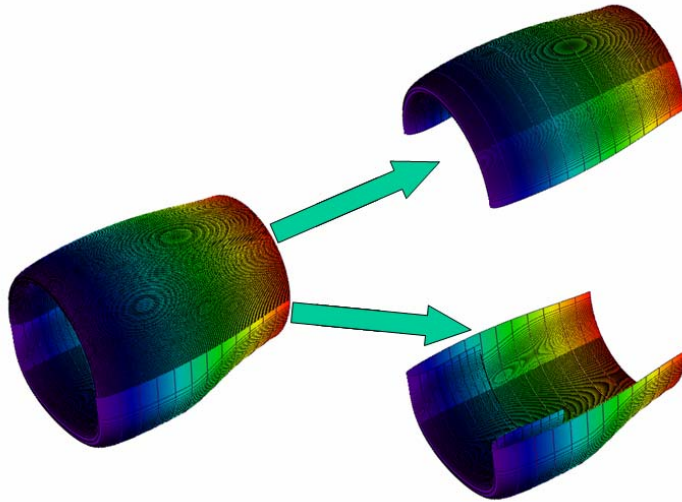


Figure 30: Total Nacelle External Shape and Inlet Geometry Definition → 15 variables

A series of cross sectional cuts through the nacelle are also shown in figure 31. Based on this example, it would appear that for aerodynamic design optimization of the external shape of a nacelle, relatively few variables would be required to capture a very large design space of realistic smooth continuous geometries.

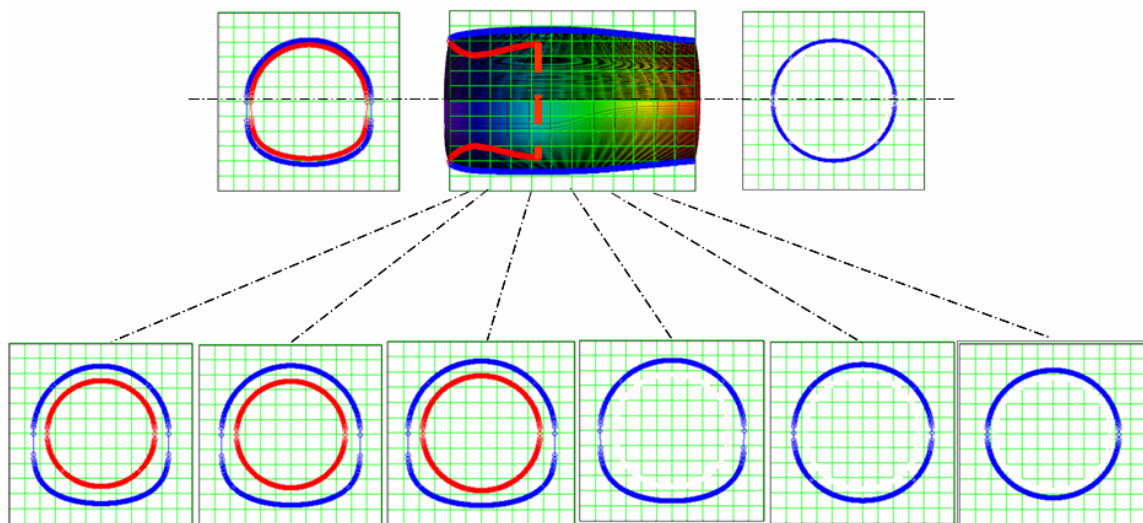


Figure 31: Nacelle Cross-Sections

## XI. 3D Wing Definition Using the CST Method

A 3D wing can be considered as a distribution of airfoils across the wing span. Consequently we can use the previously discussed class functions and shape functions to obtain analytical definitions of the wing airfoil sections and then simply distribute the analytical formulations across the wing span to completely define a wing. In this section we will first develop the analytical definition for any arbitrary wing. We will illustrate the use the methodology initially with a number of simple applications. This will be followed by an examination of application of the methodology to detailed subsonic and supersonic wings definitions.

A typical wing airfoil section is shown in figure 32. The definition of a wing airfoil section has two additional parameters relative to the previously shown airfoil definition (figure 1)

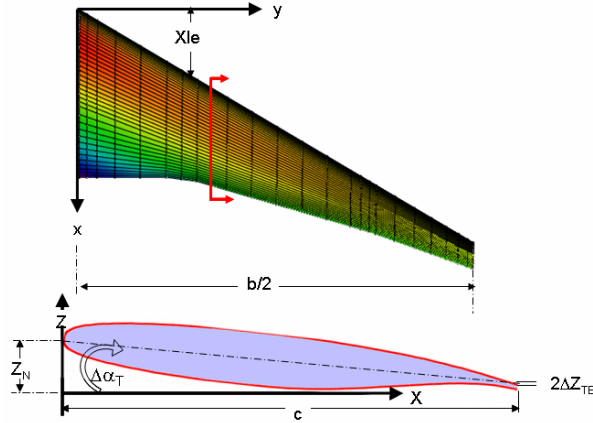


Figure 31: Nacelle Cross-Sections

The analytical definition of a local wing airfoil section is similar to the airfoil definition, (equation 1), with the two additional parameters.

$$\zeta_U(\psi, \eta) = \zeta_N(\eta) + C_{1.0}^{0.5}(\psi) \bullet S_U(\psi, \eta) + \psi [\zeta_T(\eta) - \Delta\alpha_T(\eta)] \quad (20)$$

Where:

Fraction of local chord: 
$$\psi = \frac{x - x_{LE}(\eta)}{c(\eta)}$$

Non-dimensional semi-span station: 
$$\eta = \frac{2y}{b}$$

Local leading edge coordinates: 
$$x_{LE}(\eta)$$

Local chord length: 
$$c(\eta)$$

Non-dimensional upper surface coordinate: 
$$\zeta_U(\eta) = \frac{z_U(\eta)}{c(\eta)}$$

Non-dimensional local wing shear: 
$$\zeta_N(\eta) = \frac{z_N(\eta)}{c(\eta)}$$

Equation 20 is the equation for the wing upper surface, the similar equation for the lower surface is:

$$\zeta_L(\psi, \eta) = \zeta_N(\eta) + C_{1.0}^{0.5}(\psi) \bullet S_L(\psi, \eta) + \psi [\zeta_T(\eta) - \Delta\alpha_T(\eta)] \quad (21)$$

The physical  $z$  coordinate is transformed in the shape function using an extension of the airfoil shape function procedure to derive equation 2. The corresponding shape for an airfoil section on a wing with vertical shear and local section twist is given by the equation:

$$S_U(\psi, \eta) = \frac{\zeta_U(\psi, \eta) - \zeta_N(\eta) - \psi [\zeta_T(\eta) - \Delta\alpha_T(\eta)]}{C_{1.0}^{0.5}(\psi)} \quad (22)$$

The corresponding shape function equation for the lower surface of a wing is:

$$S_L(\psi, \eta) = \frac{\zeta_L(\psi, \eta) - \zeta_N(\eta) - \psi [\zeta_T(\eta) - \Delta\alpha_T(\eta)]}{C_{1.0}^{0.5}(\psi)} \quad (23)$$

For a given wing definition, the wing upper and lower shape functions can be calculated using equations 22 and 23.

Given a wing definition as a shape function surface in the design space, the wing upper, and lower surfaces in physical space can be determined from the shape function surfaces, the local values of twist, shear and chord length as:

$$\begin{aligned} z_U(x, y) &= \left\{ \zeta_N(\eta) + C_{1.0}^{0.5}(\psi, \eta) S_U(\psi, \eta) + \psi [\zeta_T(\eta) - \Delta\alpha_T(\eta)] \right\} C_{LOCAL}(\eta) \\ z_L(x, y) &= \left\{ \zeta_N(\eta) + C_{1.0}^{0.5}(\psi, \eta) S_L(\psi, \eta) + \psi [\zeta_T(\eta) - \Delta\alpha_T(\eta)] \right\} C_{LOCAL}(\eta) \end{aligned} \quad (24)$$

Figure 32 illustrates the general process of transforming the shape function surfaces for a wing in the design space into the physical definition of the wing. The unit design space is defined by  $\psi = 0.0$  to  $1.0$ , and  $\eta = 0.0$  to  $1.0$  and therefore represents any wing planform.

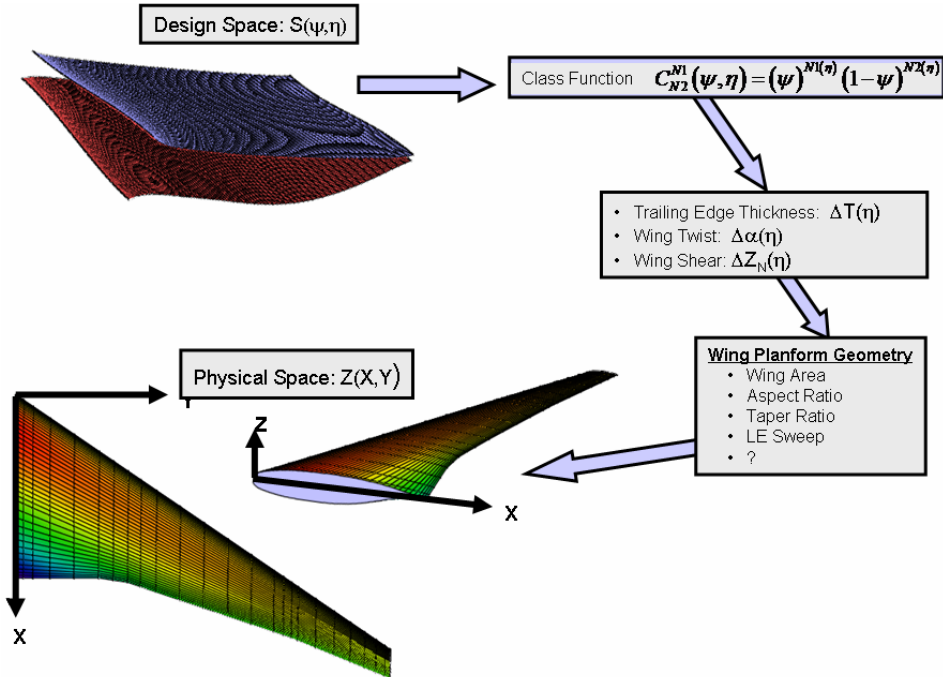


Figure 32: Transformation from Design Space to Physical Space

The class function exponents in figure 32 are shown to potentially vary with the spanwise station,  $\eta$ . For a subsonic wing the class function exponents are constant across the wing. However a supersonic wing type planform often has a highly swept inboard panel with a subsonic round nose leading edge, and a reduced sweep outboard supersonic leading edge panel with shape nose airfoils.

Figures 33 through figure 35 shows an example of process of transformation from the unit basis wing definition in the design space, into a specific detailed wing definition.

Figure 33 shows the wing section shape corresponding to a unit basis shape function surface and the effect of changing the unit shape function into the corresponding to the shape function corresponding to a constant RAE2822 type airfoil across the wing span. This would require, as previously shown in figure 12, about 11 variables to define the upper and lower surface of the airfoil.

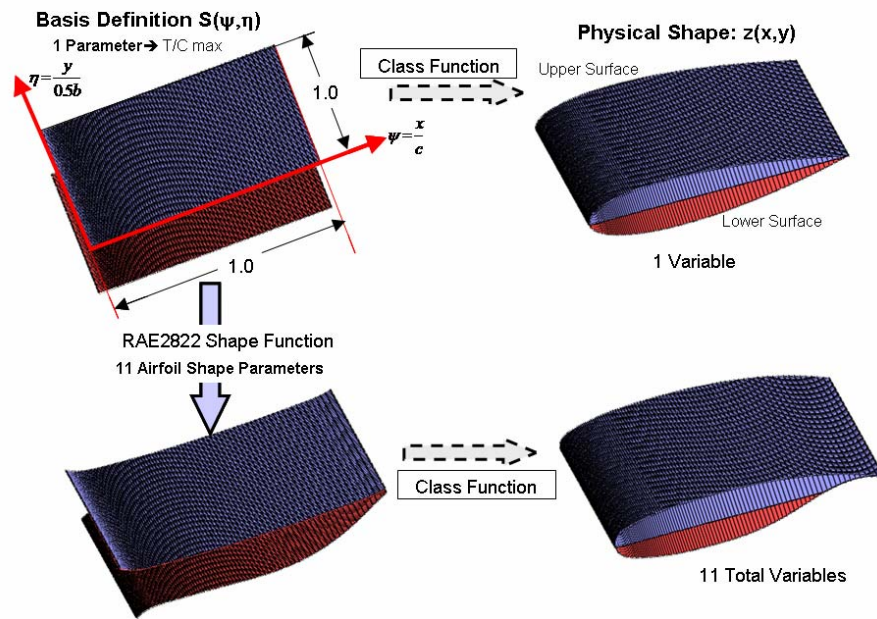


Figure 33: Parametric Wing Design Space,  $\psi, \eta, S$

The effect of including a spanwise variation of maximum thickness ratio is shown in figure 34. For this example, this represents the complete wing definition in the design space.

Figure 35 shows transformation of the wing in design space into the complete physical wing definition. The key parameters that define the wing planform and the spanwise twist distribution, are also shown.

In this example, the complete parametric cambered wing definition with spanwise variations of maximum thickness and wing twist, and specified wing area, sweep, aspect ratio and taper ratio required only a total of 19 design variables:

- Supercritical Airfoil Section (11)
- Spanwise Thickness Variation (2)
- Spanwise Twist Variation (2)
- Wing Area (1)
- Aspect Ratio (1)
- Taper Ratio (1)
- L.E. Sweep (1)

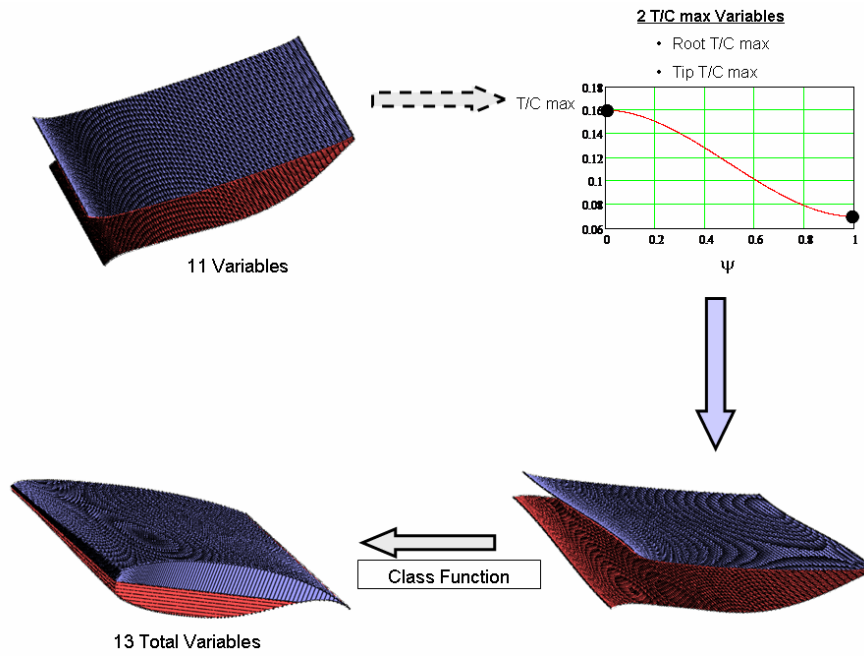


Figure 34: Incorporate Spanwise Variation of Wing Thickness

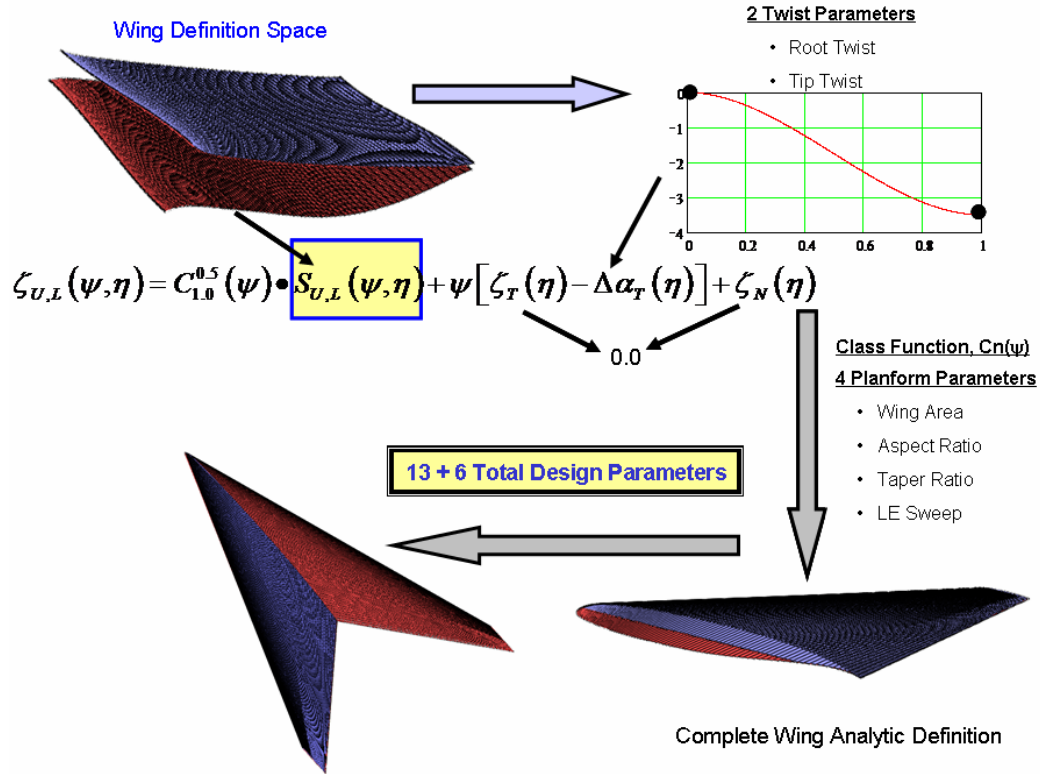


Figure 35: Complete Parametric Wing Definition

Figure 36 shows that the same design space definition of a wing, can define detailed surface geometry for a variety of wing planforms depending on the planform defining parameters. In the cases shown, the various planforms are obtained by varying wing sweep while keeping the structural aspect ratio constant.

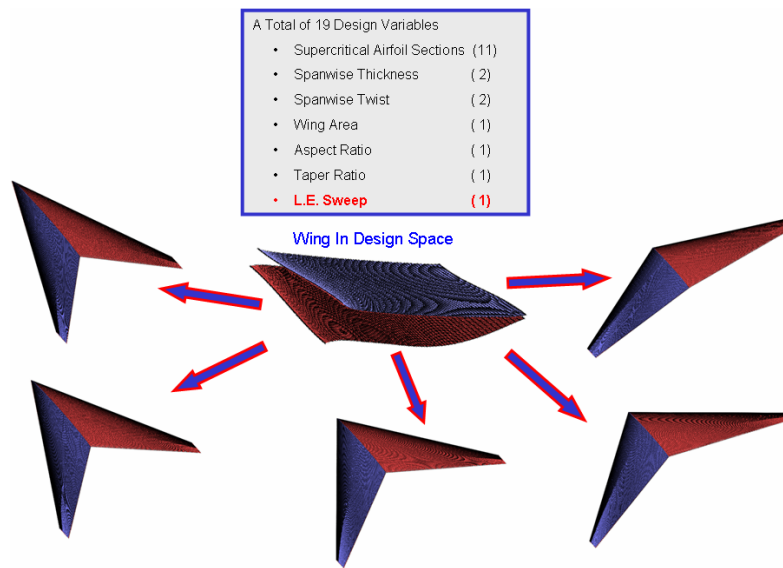


Figure 36: Parametric Wing Definition – Vary Wing Sweep

## XII. Mathematical Description of a Wing in Design Space

Similar to the shape function for an airfoil, the shape function design surface for simple wings such as shown in figure 36, is a smooth continuous analytic surface. Consequently the shape function surface can be described by a Taylor series expansion in x and y as:

$$f(x, y) = f(x_0, y_0) + \left[ \frac{\partial f}{\partial x} \Delta x + \frac{\partial f}{\partial y} \Delta y \right]_{x_0, y_0} + \frac{1}{2!} \left[ \frac{\partial^2 f}{\partial x^2} \Delta x^2 + 2 \frac{\partial^2 f}{\partial x \partial y} \Delta x \Delta y + \frac{\partial^2 f}{\partial y^2} \Delta y^2 \right]_{x_0, y_0} + \dots + \frac{1}{n!} \left[ \left( \Delta x \frac{\partial}{\partial x} + \Delta y \frac{\partial}{\partial y} \right)^n f(x, y) \right]_{x_0, y_0} + \dots \quad (25)$$

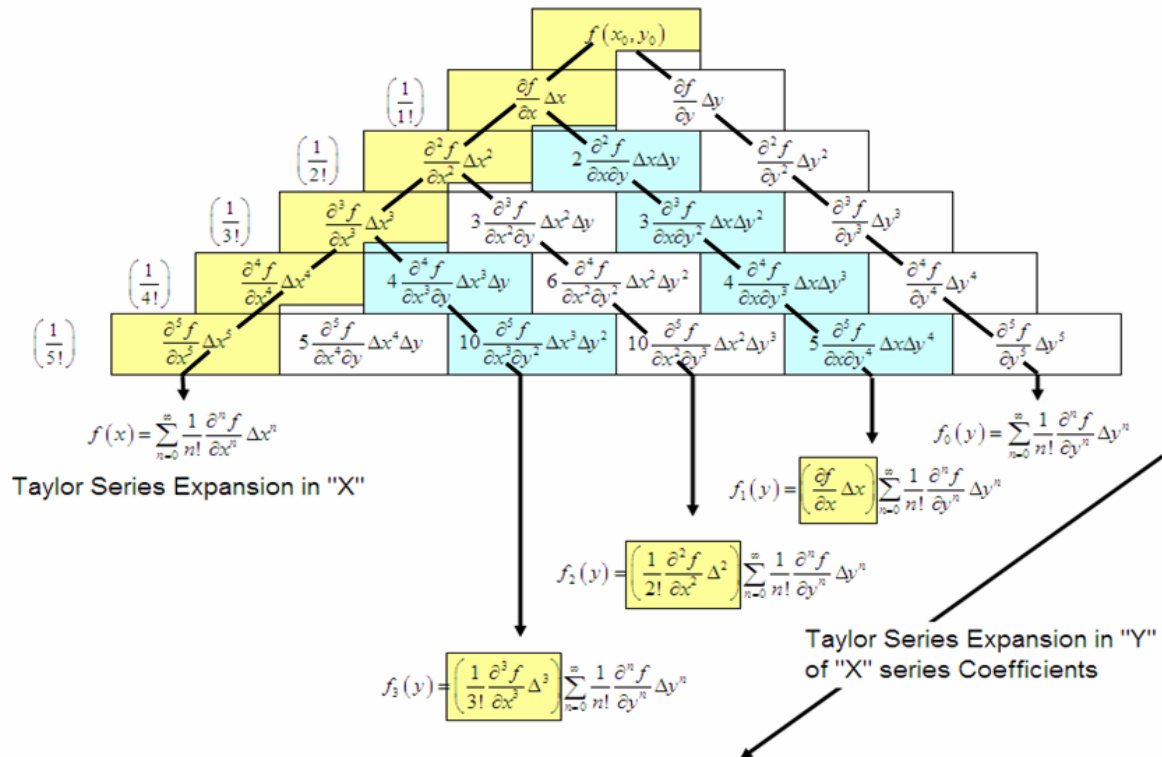


Figure 37: Taylor's Series Expansion in Two Variables – Another view

From the arrangement of the series terms shown in figure 37, it is seen that a Taylor series in x and y is equivalent to a Taylor series expansion first in the x direction, and then expanding each coefficient of the “x series” as a Taylor expansion in the y direction. In a similar manner, it can be shown that a power series in x and y is equivalent to an expansion in x followed by power series expansions in the y direction of each of the x series coefficients.

These conclusions imply that the shape function surface for a complete wing surface can be obtained by first representing the root airfoil using the previously described Bernstein polynomial approach. The complete wing shape function surface can then be defined by expanding the coefficients of the Bernstein in the spanwise direction using any appropriate numerical technique. The surface definition of the wing is then obtained by multiplying the shape function surface by the wing class function. This in essence provides a numeric scalar definition of the wing surface.

Physically this means that the root airfoil is represented by a series of composite airfoils defined by the selected Bernstein polynomial. The entire wing is then represented by the same set of composite airfoils. The magnitude of each composite airfoil varies across the wing span according to the spanwise expansion technique and wing definition objectives. For example the definition objective could be a constrained wing design optimization.

An example of the mathematical formulation of this process is shown below, using Bernstein polynomials to represent the stream wise airfoil shapes as well as for the spanwise variation of the streamwise coefficients.

The unit streamwise shape functions for Bernstein polynomial of order Nx are defined as:

$$Sx_i(\psi) = Kx_i \psi^i (1-\psi)^{Nx-i} \text{ for } i = 0 \text{ to } Nx \quad (26)$$

Where the streamwise binomial coefficient is defined as

$$Kx_i \equiv \binom{Nx}{i} \equiv \frac{Nx!}{i!(Nx-i)!} \quad (27)$$

The streamwise upper surface shape function at the reference spanwise station,  $\eta_{REF}$  is

$$Su(\psi, \eta_{REF}) = \sum_{i=1}^{Nx} Au_i(\eta_{REF}) \bullet Sx_i(\psi) \quad (28)$$

Let us represent the spanwise variation of each of the coefficients,  $Au_i(\eta)$  by Bernstein polynomials as:

$$Au_i(\eta) = \sum_{j=1}^{Ny} Bu_{i,j} \bullet Sy_j(\eta) \quad (29)$$

$$\text{Where } Sy_j(\psi) = Ky_j \psi^j (1-\psi)^{Ny-j} \text{ for } j = 0 \text{ to } Ny \quad (30)$$

$$\text{And } Ky_j \equiv \binom{Ny}{j} \equiv \frac{Ny!}{j!(Ny-j)!} \quad (31)$$

The wing upper surface is then defined by:

$$\zeta_U(\psi, \eta) = C_{N2}^{N1}(\psi) \bullet \sum_i^{Nx} \sum_j^{Ny} [Bu_{i,j} \bullet Sy_j(\eta) \bullet Sx_i] + \psi \bullet (\zeta_T(\eta) - \tan \alpha_{TWIST}(\eta)) + \zeta_N(\eta) \quad (32)$$



The similar equation for the lower surface is:

$$\zeta_L(\psi, \eta) = C_{N2}^{N1}(\psi) \cdot \sum_i^{Nx} \sum_j^{Ny} [Bl_{i,j} \cdot Sy_j(\eta) \cdot Sx_i] + \psi \cdot (\zeta_T(\eta) - \tan \alpha_{TWIST}(\eta)) + \zeta_N(\eta) \quad (33)$$

In equations 32 and 33 the coefficients  $Bu_{i,j}$  and  $Bl_{i,j}$  define the unique geometry of the wing upper and lower surfaces. Continuity of curvature from the upper surface around the leading edge to the lower surface is easily obtained by the requirement:  $Bu_{0,j} = Bl_{0,j}$

The actual wing surface coordinates can then be obtained from the equations:

$$\begin{aligned} y &= \frac{b}{2} \eta \\ x &= \psi C_{LOC}(\eta) + x_{LE}(\eta) \\ z_U(x, y) &= \zeta_U(\psi, \eta) C_{LOC}(\eta) \\ z_L(x, y) &= \zeta_L(\psi, \eta) C_{LOC}(\eta) \end{aligned} \quad (34)$$

This process of defining a wing geometry using equations 32, 33 and 34, may be considered a **scalar loft** of a wing where every points on the wing surface is defined as accurately as desired and the points are all “connected” by the analytic equations. This is in contrast to the usual wing definition of a **vector loft** of a wing which is defined as ordered sets of x,y,z coordinates plus “rules” that describe how to connect adjoining points. The common approach used to connect adjacent points is along constant span stations and along constant percent chord lines.

Figure 38 shows an example of a scalar loft of a highly swept wind tunnel wing that was used to obtain surface pressure and wings loads data for CFD validation studies<sup>3,4</sup>. The model was built using the conventional vector loft approach.

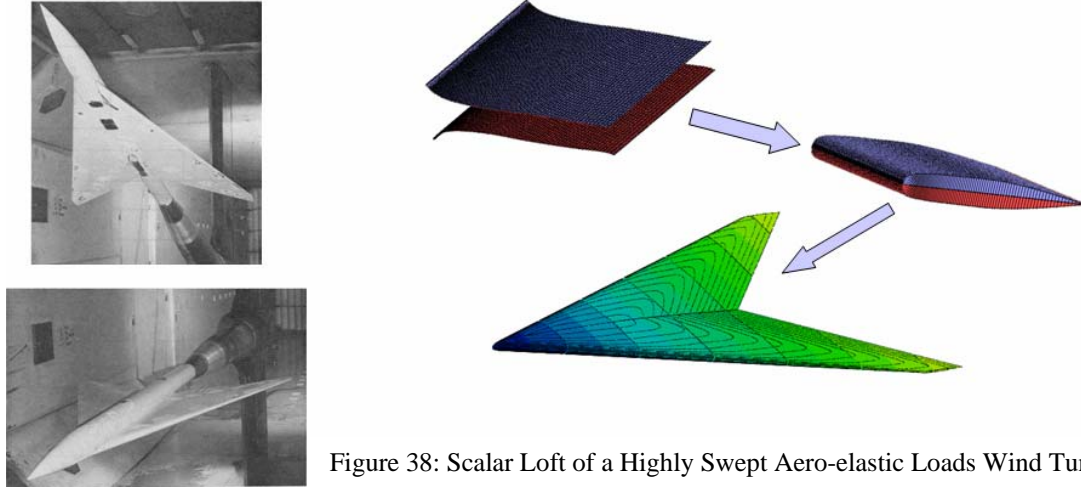


Figure 38: Scalar Loft of a Highly Swept Aero-elastic Loads Wind Tunnel Model

A analytic scalar loft of the wing can be defined by a total of 15 parameters. These include:

- BPO8 representation of the basic airfoil section → 9 parameters
- Wing area
- Aspect ratio
- Taper ratio
- Leading edge sweep



- Trailing edge thickness = Constant
- Constant wing shear ( to fit the wing on the body as a low wing installation)

The differences between the analytic wing surface definition and the “as built” wing surface coordinates were far less than wind tunnel model tolerances over the entire wing surfaces.

### XIII. Mathematical Description of a Wing With Leading Edge and /or Trailing Edge Breaks

Subsonic and supersonic aircraft wings typically have planform breaks in the leading edge (e.g. strake) and / or the trailing edge (e.g. yehudi) with discontinuous changes in sweep. Consequently, the wing surface is non-analytic particularly in the local region of the edge breaks. However, the approach of defining a complete wing geometry as previously described should be applicable. The airfoil sections across the wing can be defined by the composite set of component airfoils corresponding to the selected order of Bernstein polynomial representation. The spanwise variation of the composite airfoil scaling coefficients would be most likely piecewise continuous between planform breaks.

In order explore this concept; the geometry of a typical subsonic aircraft wing was analyzed in depth. Airfoil sections at a large number of spanwise stations were approximated by equal order of Bernstein polynomial representation of the corresponding shape functions. The adequacy of the composite representation was determined by computing the residual differences between the actual airfoil sections and those defined by the approximating Bernstein polynomials. The results are shown in figures 39 and 40.

The residual differences between the approximated and actual surface ordinates are shown in figure 39 on a scale equivalent to 3% wind tunnel model. The allowable tolerance for building a wind tunnel model of that size is typically  $\pm 0.003$  inches over the first 20% of the local wing chord and  $\pm 0.006$  over the rest of the wing chord.

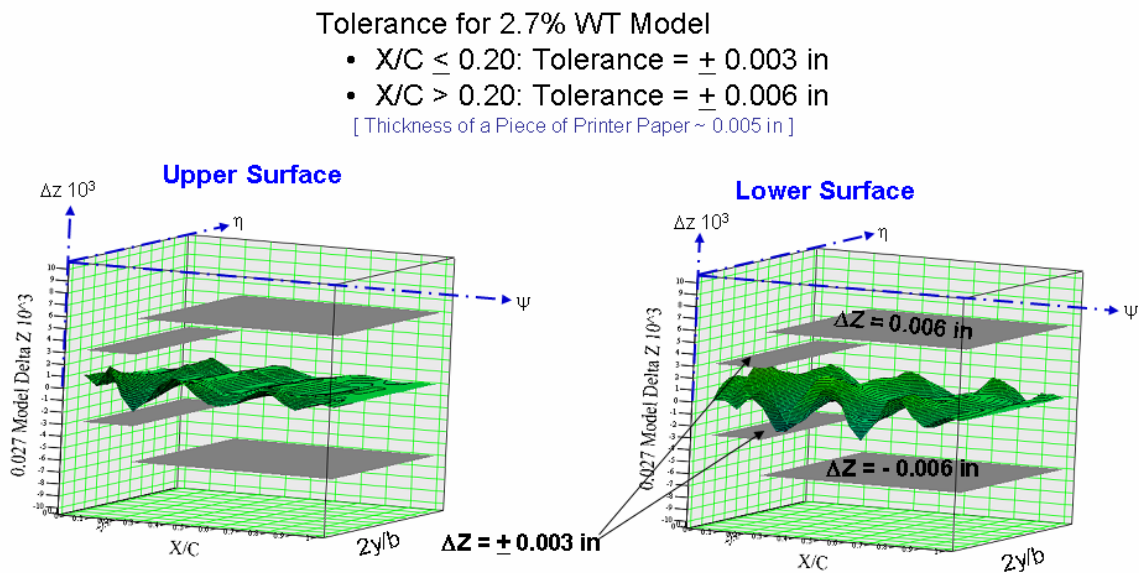


Figure 39: BPO8 Subsonic Aircraft Wing Surface Representation  $\Delta Z$  Residuals

The wing upper and lower surface residual differences are well within the wind tunnel model construction tolerances.

The shape function surfaces corresponding to wing upper and lower surfaces are shown in figure 40. The piecewise continuous nature of the surfaces associated with the planform breaks is very evident. The corresponding spanwise variations of the composite airfoil scaling coefficients ( $Bu_j$  and  $Bl_j$ ) are also shown.

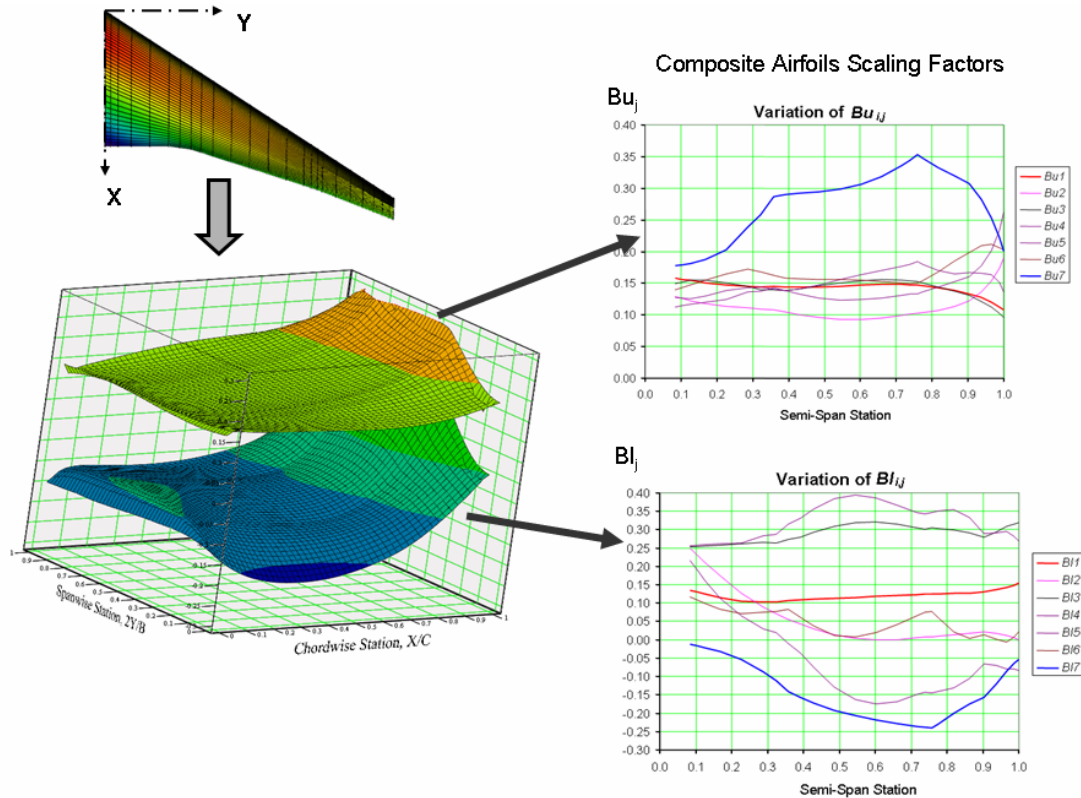


Figure 40: Spanwise Variation of the “BP” Composite Airfoil Scaling Coefficients

These results show that the spanwise variations of the Bernstein coefficients across the wing span are very regular, piecewise continuous and well behaved.

The shape function surface for a High Speed Civil Transport, Ref H, wing is shown in figure 41. This planform has a number of leading edge and trailing edge breaks. This wing has an inboard subsonic leading edge wing with round nose airfoils. Outboard of the leading edge the wing has a supersonic leading edge with sharp nose airfoils. The shape functions for this wing are also seen to be piecewise smooth and continuous.

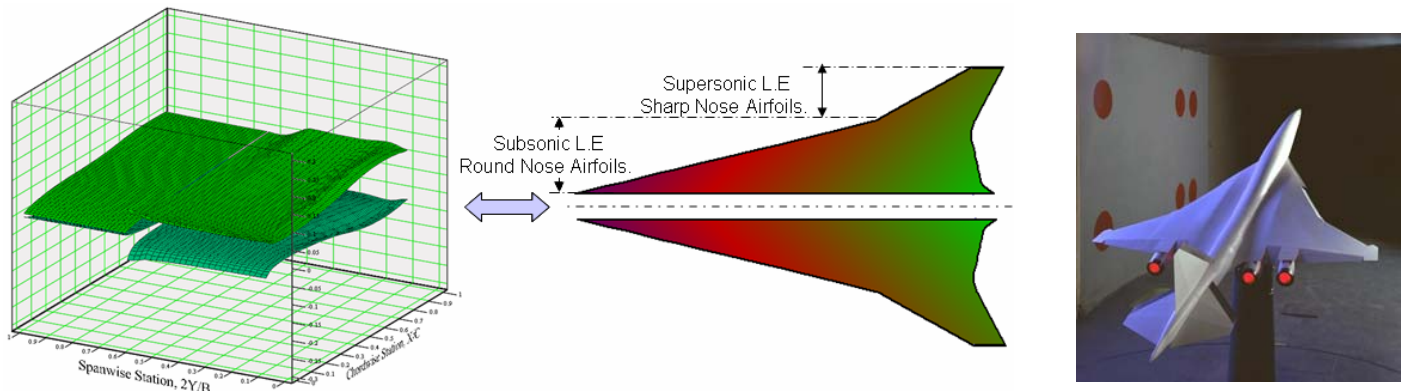


Figure 41 Shape Function for a HSCT Supersonic Wing – Ref H

## XIV. Summary and Conclusions

- The Class function / Shape function Transformation, “CST”, geometry representation method was presented, (eqn. 7, fig. 2).
- The class function with a unit shape function was shown to define fundamental classes of airfoils, axi-symmetric bodies, and axi-symmetric nacelles geometries (eqn. 6 to 6.7, fig.14). The shape function defines unique geometric shapes within each fundamental class.
- Examples were shown of a number of different methods to use the shape function for parametric airfoil modification or design (figs. 3, 4 5)
- The fundamental mathematical simplicity of using the shape function for geometry representation was shown. In the case of round nose geometries, the shape function eliminates the numerical leading edge singularities in slopes, 2<sup>nd</sup> derivatives and the large variations in curvature over the entire surface of the geometry. (fig. 13)
- The use of Bernstein Polynomials was shown to be an attractive and systematic technique to decompose the basic unit shape into scalable elements corresponding to component airfoils, (figs. 8, 9, Ref.1). This technique:
  - Provides direct control of key design parameters such as leading edge radius, continuous curvature around a leading edge, boattail angle and closure to a specified thickness.
  - Captures the entire design space of smooth airfoils, axisymmetric bodies and nacelles
  - All smooth airfoils, axisymmetric bodies and nacelles are derivable from the unit shape function and therefore from each other.
- The “CST” method was shown to be applicable to the definition of body cross-section geometries. A number of cross-sectional geometries corresponding to various class functions were shown,(figs. 16, 18)
- Three dimensional bodies in general can be represented as a distribution of fundamental cross-sectional shapes. The Class function / Shape function Transformation geometry representation methodology, CST, can be used to describe both the fundamental cross-sectional shapes as well as the distribution of the fundamental shapes along the primary body axis, (figs. 20 to 26)
- Examples of using a few design variables to develop detailed design definitions of the external shape and inlet of a non-symmetric nacelle and for a number of three dimensional wings were shown, (figs. 30, 35, 36).
- The concept of “analytic scalar definitions of wing surfaces” was introduced. With this approach, the wing surfaces sectional shape functions are represented by a Bernstein polynomial. The selected order of Bernstein polynomial effectively defines a set of composite airfoils for constructing the wing surface definitions. The coefficients of the Bernstein polynomials can then be mathematically expanded in the spanwise direction to define wing upper and lower shape function surfaces. The shape function surfaces are then easily transformed into the physical wing geometry, (eqns. 32,33,34, fig.38)
- The application of analytic scalar wing definitions to planforms with leading edge and / or trailing edge breaks was discussed and illustrated by examples, ( figs. 40,41).
- The analytic CST geometry representation methodology presented in this report provides the unified and systematic approach to represent a wide variety of 2D and 3D geometries encompassing a very large design space with a relatively few scalar parameters, (fig 42).

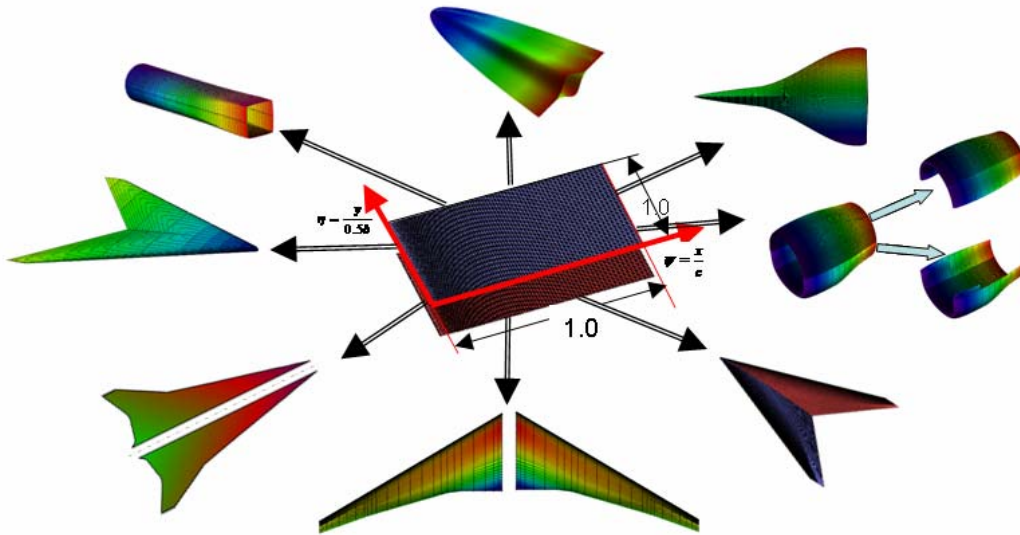


Figure 42: CST Design Methodology

## XV. References

1. Kulfan, B.M, Bussoletti, J.E., "Fundamental Parametric Geometry Representations for Aircraft Component Shapes". AIAA-2006-6948, 11th AIAA/ISSMO Multidisciplinary Analysis and Optimization Conference: The Modeling and Simulation Frontier for Multidisciplinary Design Optimization, 6 - 8 September 2006
2. Sobieczky, Helmut, "Aerodynamic Design and Optimization Tools Accelerated by Parametric Geometry Preprocessing ", , European Congress on Computational Methods in Applied Sciences and Engineering, ECCOMAS 2000
3. Manro,M.E., Percy J. Bobbitt, P.J. and Kulfan, R. M., "The Prediction of Pressure Distributions on an Arrow Wing Configuration Including the effects of Camber Twist and a Wing Fin", NASA CP-2108 Paper No 3 pages 59 to 115, November 1979
4. Wery, A.C.and Kulfan, R. M., "Aeroelastic Loads Prediction for an Arrow Wing - Task II Evaluation of Semi-Empirical Methods", NASA CR-3641 March 1983